Hes·so VALAIS WALLIS
Haute Ecole d'Ingénierie
Hochschule für Ingenieurwissenschaften

Hes·so

Degree Programme
Systems Engineering

Major Power & Control

Bachelor's thesis
Diploma 2022

Nathan Sierro

Study, sizing, and setting of a DAB converter

Professor
Philippe Barrade

Expert
Name Surname

Submission date of the report
cf. thesis form (16.09.2022)

HES-SO Valais-Wallis • rue de l'Industrie 23 • 1950 Sion
+41 58 606 85 23 • hei@hevs.ch • www.hevs.ch/hei

Filière / Studiengang **SYND**	Année académique / *Studienjahr* **2021-22**	No TB / *Nr. BA* **PC/2022/95**
Mandant / *Auftraggeber* ☐ HES—SO Valais ☐ Industrie ☒ Etablissement partenaire *Partnerinstitution*	Etudiant / *Student* **Nathan Sierro** Professeur / *Dozent* **Philippe Barrade**	Lieu d'exécution / *Ausführungsort* ☐ HES—SO Valais ☐ Industrie ☒ Etablissement partenaire *Partnerinstitution*
Travail confidentiel / *vertrauliche Arbeit* ☐ oui / ja ☒ non / nein	Expert / *Experte* *(données complètes)*	

Titre / *Titel*

Etude, dimensionnement et réglage d'un convertisseur DAB

Description / *Beschreibung*

Dans le cadre de ses activités de recherche, l'institut CITCEA-UPC de l'Université Polytechnique de Catalogne souhaite lancer le développement d'un convertisseur de type "Dual Active Bridge", pour des applications de conversion DC/DC basse tension. Le but du projet est d'analyser le fonctionnement d'un tel convertisseur, de le dimensionner et de pré-valider le comportement de ce dispositif par simulation. Son contrôle devra être identifié et testé par simulation. Selon le temps à disposition, il peut être envisagé de tester ce contrôle et la structure DAB sur les simulateurs temps réels du Laboratoire d'Electronique Industrielle de la HES-SO Valais/Wallis.
Si ce projet comporte une composante forte liée à une structure de conversion de l'électronique de puissance qu'il faudra analyser puis dimensionner, une difficulté principale sera liée aux contraintes et au dimensionnement associé du transformateur moyenne fréquence qu'une telle structure exige. D'autre part, une analyse sérieuse du comportement fonctionnel d'une structure DAB devra être entreprise pour identifier la structure de réglage associée. Cette dernière devra non-seulement prendre en compte la gestion du flux de puissance au sein du DAB, mais également la gestion de la magnétisation du transformateur.
Objectifs / *Ziele*

— Etude du fonctionnement d'un convertisseur DAB, analyse des spécifications.
— Développement d'un modèle de convertisseur– Fonctionnement en boucle ouverte – Analyse des contraintes et éléments dimensionnement pour la structure complète (composants de puissance et transformateur).
— Mise en œuvre d'une description fonctionnelle du convertisseur– Définition d'une structure de réglage associée.
— Selon le temps à disposition : implémentation d'un modèle de convertisseur DAB sur simulateur temps réel, et tests de la structure de réglage sur plateforme de réglage digitale (DSP).

Signature ou visa / *Unterschrift oder Visum*	Délais / *Termine*
Responsable de l'orientation / *Leiter der Vertiefungsrichtung:* F. Moghaddam ..... [1] Etudiant / Student :	Attribution du thème / *Ausgabe des Auftrags:* **16.05.2022** Présentation intermédiaire / *Zwischenpräsentation*: **20-21.06.2022** Remise du rapport final / *Abgabe des Schlussberichts:* **16.09.22, 12:00** Défense orale / *Mündliche Verfechtung:* **Semaine/Woche 40**

[1] *Par sa signature, l'étudiant-e s'engage à respecter strictement la directive DI.1.2.02.07 liée au travail de diplôme.*
Durch seine Unterschrift verpflichtet sich der/die Student/in, sich an die Richtlinie DI.1.2.02.07 der Diplomarbeit zu halten.

Rapport reçu le / *Schlussbericht erhalten am* …….. Visa du secrétariat / *Visum des Sekretariats* ……..

Hes·so VALAIS WALLIS

Haute Ecole d'Ingénierie
Hochschule für Ingenieurwissenschaften

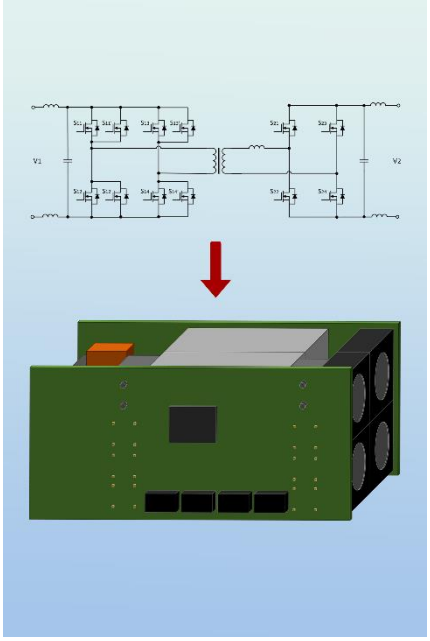

Study, sizing, and setting of a DAB converter

Graduate Sierro Nathan

Objectives

This thesis focuses on an isolated bidirectional DC (IBDC) converter connected on a smart grid, especially a Dual Active Bridge (DAB) converter. The goal is to study this topology, size the converter and analyse the power devices.

Methods | Experiences | Results

A state of the art of isolated bidirectional DC (IBDC) converter has been done to understand and select the topology for this converter. The DAB topology has been selected. Its modulation scheme and how power is transferred through the converter have been studied. Knowing the power losses generated by power devices, a selection of component from the market have been made. Switching devices are the key point of this thesis. With an unstable market, they had to be selected and studied to ensure to create less losses as possible. Referring to a converter from a project of European Union created in the partner school, some analyses, as thermal analysis, have been done to define which component fit with the specified application. The sizing of the elements allowing the dissipation of the power losses have been made and a study of filters added to the converter was investigated to attenuate the currents and the harmonics generated before and after the converter. A final global analysis was done to control if the objectives of high-power density, galvanic isolation and high efficiency have been achieved.

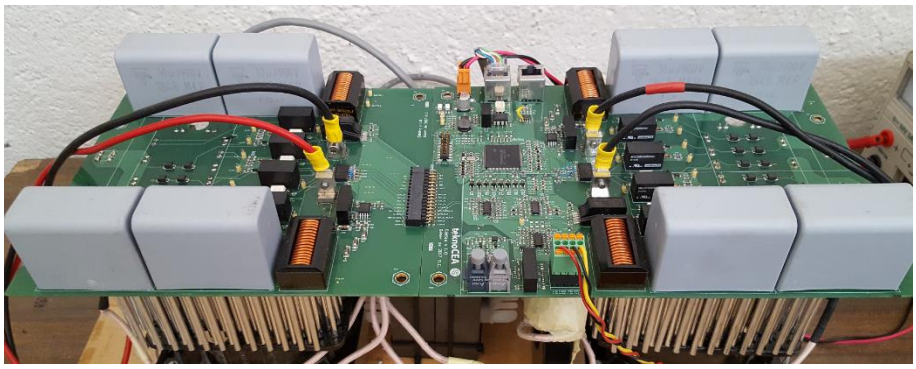

The thesis is based on this example of real converter and focuses on the power devices optimization. Real converter used for the project « RESOLVD » of European Union.

Bachelor's Thesis
| 2022 |

Degree programme
Industrial Systems

Field of application
Power and Control

Supervising professor
Dr Philippe Barrade
philippe.barrade@hevs.ch

Partner
Dr Daniel Montesinos-Miracle
daniel.montesinos@upc.edu

List of abbreviations

Symbol	Description	Page

1

1-S
Single-Stage 66

2

2-S
Dual-Stage 66

A

AC
Alternative Current 20, 21, 70

C

C_{IN}
Capacitor of input filter 56, 57

C_{OUT}
Capacitor of output filter 57

D

d
Voltage ratio 19

DAB
Dual Active Bridge 1, 21, 22, 23, 24, 25, 26, 32, 49, 63, 66, 67

DC
Direct Current 15, 17, 18, 19, 20, 21, 25, 26, 36, 38, 40, 41, 57, 66, 70

DES
Distributed Energies Sources 15

DPS
Dual Phase Shifting 28

E

EV
Electrical Vehicle 14, 15, 62

F

f_{sw}
Switching frequency 19

H

HF
High Frequeny 20, 22, 24

HV
High Voltage 18, 19, 66

I

IBDC
Isolated Bidirectional DC converter 17, 20, 21, 66

L

N

P

Q

R

S

T

V

Z

Δ

Contents

List of figures

List of tables

1
Context

The current energy context is constantly changing. Political decisions to reduce the carbon footprint of our society and particular geopolitical situations such as the war in Ukraine mean that supply and demand are constantly being challenged.

In Europe, the European Commission has set up the Green Pact for Europe [1], which aims to find a balance between the emissions created that contribute to global warming and the emissions absorbed. The goal is to reduce CO^2 emissions by 55% for 2030 and become carbon neutral for 2050 through the creation of renewable energy, more efficient consumers, cleaner transport, greener farms, and a circular economy. Also, a ban on the sale of internal combustion passenger cars is planned for 2035. This pact aims to accelerate the implementation of work to achieve the goals of the Paris agreements. However, each country will meet these targets in its own way. While Germany decides to do so while betting to get out of nuclear power in 2022, France builds new nuclear power plants in order to reduce other fossil fuels. In Spain, which is considered to be on an energy island with Portugal, the strategy is largely focused on the development of wind and photovoltaic farms. In 2021, it reached a record of 47% of renewable energy in its electricity mix, of which 23% comes from wind power. Switzerland, which is not directly affected by the European Commission's decisions, is also planning to be carbon neutral by 2050 while phasing out nuclear power. Despite being at the centre of Europe, a gateway for various imports/exports between the countries around it, this one faces the risk of an energy blackout in the coming winters, following disagreements with the EU. It must also find solutions to boost its production of renewable energy, which already accounts for 58% of its electricity mix in 2021.

The stakes throughout Europe are therefore high and the time to achieve this is already close. Adding to this the unstable geopolitical context in Eastern Europe with the Russian invasion of Ukraine, the European Commission has therefore put in place the REPowerEU plan [2]. It is a response to the difficulties and disruption of the global energy market caused by this war. The goals are to save energy, produce clean energy and diversify energy producers. This plan is supported by financial and legal measures for the construction of new infrastructure and the new energy system that Europe needs. As many European countries are dependent on Russian gas and oil imports, the aim is to achieve carbon neutrality without Russian resources.

Finally, many changes are expected, particularly in the electricity network, which was largely created after the Second World War. Decentralisation of producers is necessary with the addition of micro producers such as wind, photovoltaic or micro hydro. The grid is being led to change and to be constituted of sub-grids, with more consumers such as the expansion of electric vehicles (EVs), which must be able to be of a different nature and therefore meet the needs of alternating current or direct current. This new type of electricity network, known as the "smart grid", must also be secure and affordable so that it can be easily integrated into people's daily lives.

2
Summary

This thesis deals with a model of distributed energy resource conversion in a smart grid, represented in Figure 2.1. Power electronics can be considered as a key technology for the realisation of these networks, where power quality and security are the most important points. In fact, in order to adapt to the new producers and consumers, which are essential to Europe's new energy strategies, all of which are of a different nature, this type of network must be very flexible in the supply of energy. These distributed energies sources (DES) are interconnected to the grid via electronic converters. As each electrical load contains an electronic power circuit/converter, the total electrical energy produced and consumed is converted and shaped. This means that it is important that these conversions are done with a maximum of efficiency, knowing that the new generators do not have a very high efficiency due to their variable energy density depending on the conditions (wind, sun, etc...) compared to the traditional generation plants. Also, these converters will have to be particularly reliable in the future because the expansion of power electronics in the distribution/residential level will only increase. Its widespread use in the grid will also allow greater control of the grid and its stability.

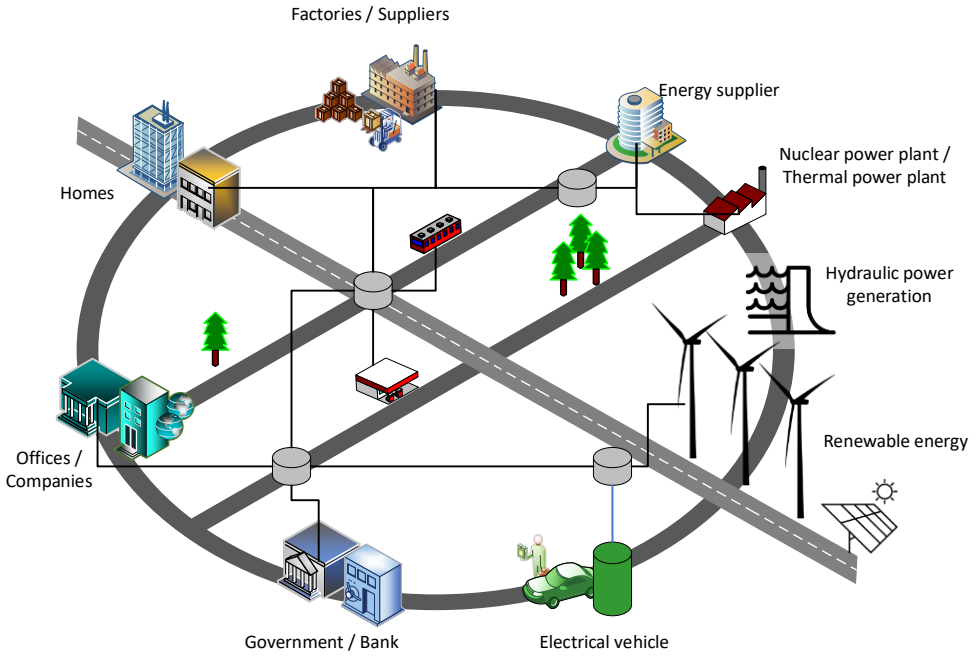

Figure 2.1 : Smart grid representation

This work focuses particularly on DC energy conversion. Indeed, photovoltaic panels, electric vehicles (EVs), fuel cells or batteries for local storage are some of the technologies that all operate on DC and contribute to the achievement of Europe's targets. These

emerging technologies are both producers and consumers, which creates a challenge for converters that must be able to transfer power in both directions. Also, galvanic isolation is becoming a mandatory safety feature in this type of network. It is important to note that smart grids can initially be installed in support of traditional grids and therefore through converters. They are therefore to be considered as important connection points between different networks and different types of energy. The criteria of primary importance are power density, i.e., the passage of high power in a small module, especially in the automotive sector, and cost effectiveness.

As mentioned, the trend to design converters in a small volume that can transfer high power density dates back a long time. When designing a converter, the important points are minimising the volume and therefore maximising the power density. Weight minimisation can also be important when it comes to a vehicle to ensure lower consumption. Also, minimisation of losses with maximum efficiency at the lowest possible cost and high reliability are to be considered. The study and design of these converters must take these objectives into account in order to be able to offer efficient and competitive products on the market.

This work is a following adaptation of the « RESOLVD project » [3], which concern the converter studied. Indeed, this converter has been sized and tested for specific applications and has been approved, but this thesis has to investigate some possibilities of improvements, especially in the power devices research.

3
Objectives

As stated earlier, this work focuses on DCDC conversion and therefore the isolated bi-directional DCDC (IBDC) topology meets the criteria of major importance and requirements for the type of network in which it must operate. The focus of this work is on this type of converter connected to the electrical network at the distribution/residential level and more particularly for a back-up in case of energy shortage or stabilisation of network disturbances. It is therefore a question of installing a converter between a DC network and a battery.

The study in this thesis is carried out only on this converter and therefore does not consider the nature of the network as a whole, for example the integration of filters upstream or not on other elements surrounding it. Therefore, the product has to adapt to any particularities of the DC network in which it can be installed.

> *"The main objective of this thesis is to study the design of the topology of an IBDC and to size it to best fit in the specific environment described, by analysing it."*

In general, such a study that leads to the design of a converter is carried out in several stages, each of which defines objectives that correspond to the nature in which the converter evolves and also serve the main objective sought by Europe, which is to reduce global energy consumption. These stages are as follows:

1. Determine the application and specifications for which the converter has to work
2. Study the existing topologies and define which one can be adapted to the application
3. Know the specific characteristics of this topology
4. Define its modulation scheme and its components
5. Model, size and analyse the electronic components
6. Carry out a global analysis of the converter and compare the results with the objectives defined by the application

By framing the project in this way, it is easy to observe its progress and to validate certain stages as they occur.

The sizing of a converter as a whole, as regards the understanding of each equipment in a precise way, taking a lot of time, this thesis focuses on the power devices (semiconductors and their modulation) and not on the magnetic part such as the sizing of the transformer allowing the galvanic insulation, which are relative to the project [3]. Nevertheless, only filters that can be quickly dimensioned are considered.

4
Application and its specifications

4.1 The application

This work investigates a particular single-phase, bi-directional DC-DC converter that allows power to be transferred between a distribution network at the residential level and a battery in a smart grid. At this level, the grid consists of different elements, several converters connect to a main DC high voltage line. These converters serve as interfaces between producers (Fuel Cell, Electrical Generators, ...) and consumers (Air conditional, Electrical Motors, ...). This study focuses on the bi-directional converter between the HV DC bus and the LV DC BUS, thus for the use of the battery in low voltage. This battery can have several uses. Firstly, it can be used as a back-up battery in the event of a standard blackout on the residential network. It can therefore take over the power source and serve as a back-up service to avoid a power cut for residents. A second use is to be able to charge the battery when the price of electricity is low and to reinject it into the grid when the price is higher. A final utility, which is expected to become increasingly important, is the potential to stabilise grid disturbances. Since electricity consumption is not linear and constant at all times of the day, the battery could provide for needs at critical times of the day. But also, given the rise of new generators such as wind turbines and photovoltaic panels, the disruptions they bring to the grid are large and very irregular. This battery can also be used to compensate for grid disturbances. The bi-directional converter is therefore necessary to transfer power according to the state of the grid and the electricity market. An application that is intended to be multiple and flexible.

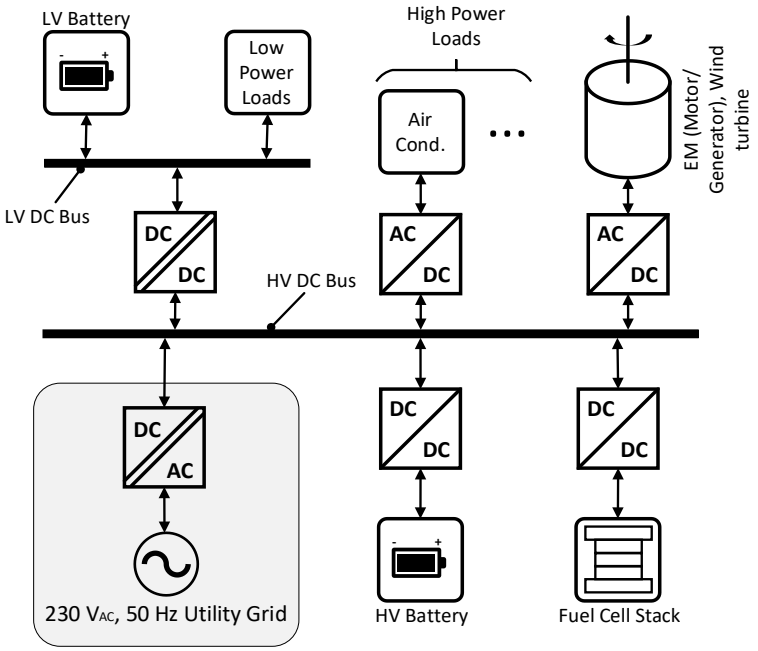

Figure 4.1: Electrical power system architecture in which involve the converter studied

This architecture can consider different elements of the smart grid for users and producers. This grid can be composed of a high voltage DC Bus, where different converters are connected to transfer energies from different

producer to different consumer. This smart grid is as well connected to the well-known main utility grid by a converter. It is as well composed of a low voltage DC Bus, which allows low batteries to be connected in. The converter studied for this thesis is the one which interconnected the two DC Buses. As it is possible to see, this converter has a galvanic isolation and need to be able to transfer energy in two directions.

4.2 Specifications

In order to design such a converter to fit the environment required above, the specifications defined by this network must be considered. The converter must therefore meet the following stated objectives:

Description	**Symbol**	**Value**	**Unit**
Rated power	P (= P_{B1} = P_{B2})	20	kW
Rated power for sizing (+20%)	P (= P_{B1} = P_{B2})	24	kW
Voltage on port 1 – LV DC Bus	V_{HF1}	240	V
Voltage on port 2 – HV DC Bus	V_{HF2}	800	V
Transformer ratio	$n_1 : n_2$	3 : 1	-
Voltage ratio {d = (V_{HF2}/ (V_{HF1}*n1n2))}	d	1,11	-
Frequency	f_{sw}	40	kHz

Table 1: Specifications of the converter

These values have to be respected in order to achieve a converter that fits the network. In order to ensure the safety of the converter, 20% is added to the desired electrical transfer power. This allows for a slightly more robust design that guarantees operation without destroying the equipment during an overload.

Some additional conditions are also necessary to achieve the objectives of the ecological ambitions:

Additional requirements
• Galvanic isolation • Bidirectional power flow capability • High conversion efficiency (η > 95 % at the nominal operating point) • High power density • Autonomous cooling • Semiconductors switching devices MOSFETs (SiC if possible)

Table 2: Additional requirements necessary for the converter

The overall mechanics of the converter are taken from the existing project that have worked well in this way [3]. Therefore, the choice and size of certain components, such as radiators and fans, are defined in advance.

5
State of the art

When designing a converter, the first thing to consider is which topology may be appropriate to meet the requirements specified in Chapter 4. Since there is a wide variety of topologies for single-phase, bi-directional, isolated DC-DC converters, it is complicated to make a complete study of each of them and their options in order to determine which one fits. Therefore, it is necessary to rely on the literature [4], which is based on designs that have already been carried out and studied, and to select some of them that should correspond to the desired application.

The purpose of this chapter is to outline the different topologies of IBDC converters that can possibly meet the objectives outlined in the previous chapter. Section 5.1 explains the different Isolated Bidirectional DC Converters that exist, expressing their strengths and weaknesses as well as their topology. Then section 5.2 develops the choice of the converter based on the specifications and requirements.

By this approach, based on already approved implementations, the following steps concerning the modelling of the converter topology, the electrical circuit model and its modulation scheme can be defined simply.

5.1 Existing IBDC topologies

In general, the advantages offered by bi-directional isolated DC converters, such as their galvanic isolation through safety transformers and their ability to transfer power flows in both directions, all with high power density, are well known. Their component parts are generally the same depending on the topology. An IBDC converter is therefore made up of the following parts, see Figure 5.1:

1. Upstream and downstream filters to smooth the voltage and current to ensure a clean signal for the conversion. These can be achieved by using capacitors or inductors.
2. DC-AC/AC-DC converter modules converting the DC signal to high frequency AC for the transformer. These two converters allow bi-directional power flow. They can be composed in different ways which will be presented below.
3. It is possible to add HF networks allowing energy storage capacity in the HF AC part to modulate the switching current waveforms in order to reduce switching losses. These are not always necessary but may be present in case of transformer disturbances. They are in the form of additional capacitors or inductors.
4. An HF transformer is necessary if the mention of galvanic isolation is required. As an option that is becoming more and more desired, the transformer allows the two parts of the converter to be isolated. Also, it can supply different voltages to the primary and secondary. The higher the operating frequency of the transformer, the smaller its size can be.

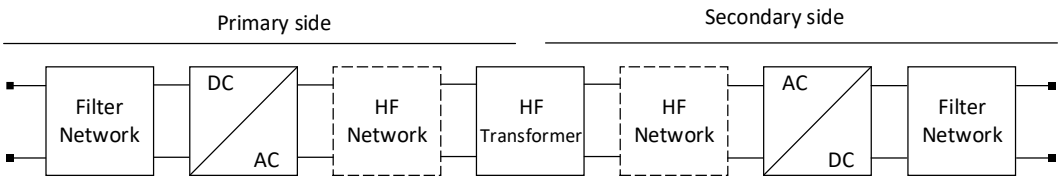

Figure 5.1: Different parts of an IBDC converter

IBDC topologies can be classified into subcategories; Single-Stage, Dual-Stage topology or according to the number of semiconductors. Also, a distinction is made if the converter is resonant or not.

5.1.1 Dual-Stage topologies

The Dual-Stage topology corresponds to the series connection of converters. For example, a PFC rectifier to rectify AC line voltage to DC voltage or vice versa, followed by a boost converter to increase the voltage level. This sequence allows the signal to be modelled as required to perform a conversion. They are generally used to cover applications requiring wide input and output voltage ranges. In this case, it would be necessary to add a DC-DC converter between the filter and the AC converter. However, the addition of a converter generates more power losses than a single converter. Therefore, when the objective is to have as little loss as possible, this topology is not the most suitable.

5.1.2 Single-Stage topologies

The Single-Stage topology is more efficient as long as it contains a minimum of components. There are different ways to create a single-stage converter. They can be divided into three groups, see Figure 5.2; topologies with a low number of switches, topologies with Double Bridge without resonant network and resonant DAB.

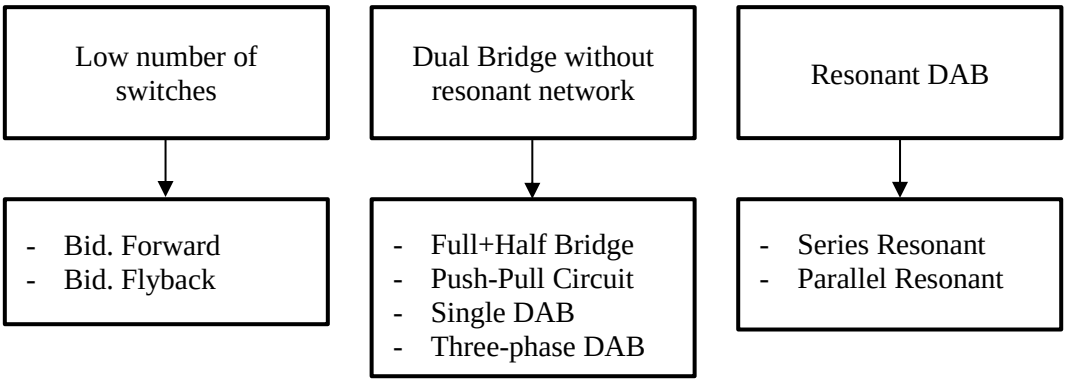

Figure 5.2: Topological Single-Stage classification

5.1.2.1 Low number of switches

The first type of topology corresponding to the Single-Stage is the one with the smallest number of switches. For example, bidirectional converters such as Forward or Flyback, see Figure 5.3, as well as other variants, contain few components and allow bidirectional power transfer with galvanic isolation, but this is for maximum powers of 2 [kW]. These topologies are therefore not suitable for high power applications.

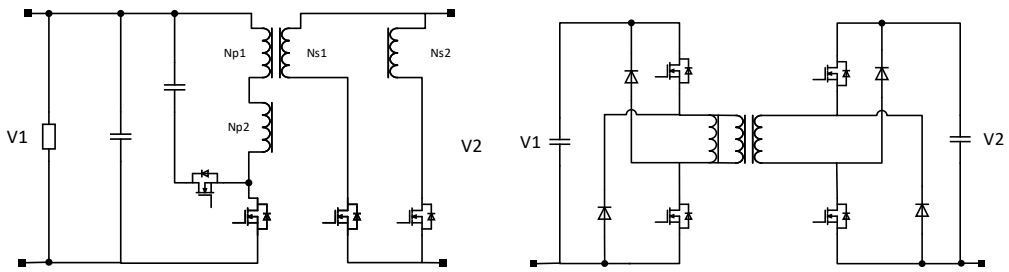

(a) Bidirectional forward (b) Bidirectional flyback

Figure 5.3: IBDC topologies with less switches

5.1.2.2 Dual Bridge Converters without Resonant Network

The second type of topology for the Single-Stage is the so-called Dual Bridge without resonant network. It can be formed by full bridges, half-bridges, or possible variations with passive components.

1. The first possibility for this type of topology is Single Dual Active Bridge (DAB), see Figure 5.4. This is interesting for its low component count and uniform current distribution across the different power devices. Its operating principle is based on a phase shift between the input and output voltages, which allows energy transfer. The opportunity to operate under soft switching conditions is also an advantage of this type of topology. Often an inductor in series with the stray transformer inductor is added, or the stray transformer inductor itself is used to control the HF current.

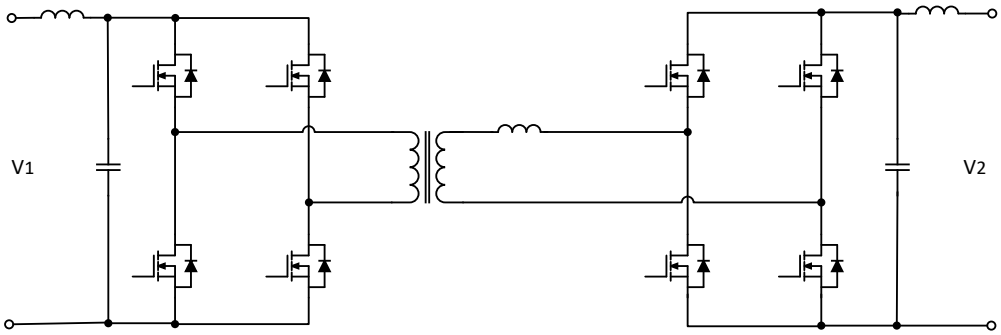

Figure 5.4: Dual Active Bridge (DAB) topology

2. The second possibility is a variation of the first, Three-phase Dual Active Bridge (DAB), see Figure 5.5. This version allows a smaller RMS current to flow through the components. It is controlled by a similar single-phase shifting switching strategy. The disadvantage is that more components are required.

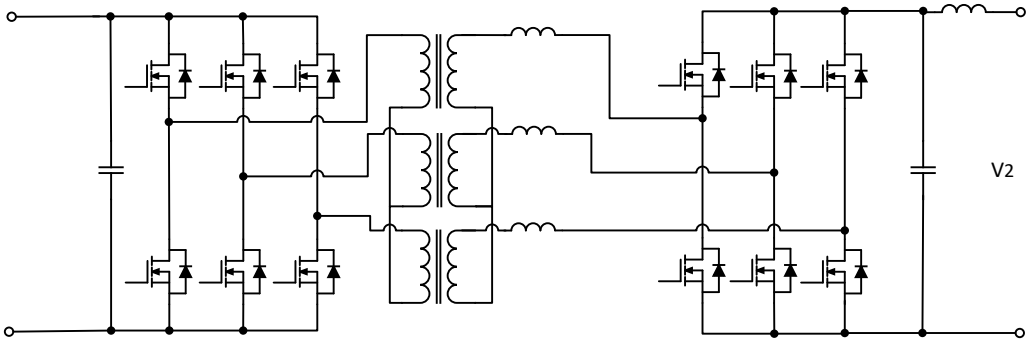

Figure 5.5: Three-phase Dual Active Bridge (DAB) topology

3. The last possibility is the Bidirectional Isolated Full Bridge Converter, see Figure 5.6. This time the high voltage bridge is controlled as a voltage source and the low voltage bridge is controlled as a buck converter. Indeed, the parasitic inductance of the transformer is reduced, and an additional inductance is added on the low voltage side. The RMS current in the capacitors is lower. However, the inductance in series with the parasitic inductance of the transformer emits voltages spikes at each switching period.

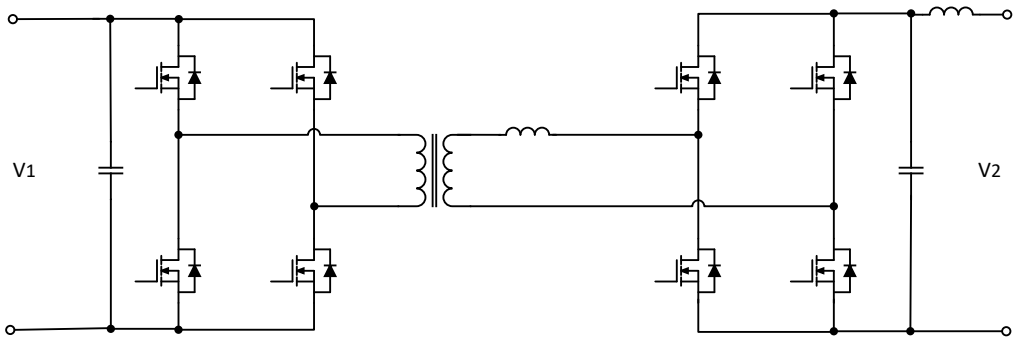

Figure 5.6: Bidirectional Isolated Full Bridge Converter

These possibilities can be implemented with full bridges, but also with different variants on each bridge. The most commonly used alternatives are push-pull or half-bridge topologies.

5.1.2.3 Dual Bridge Converters with Resonant Network

Finally, the third type of topology for Single-Stage is called Dual Bridge Converters with Resonant Network. Topologies such as LLC or LCC are currently widely studied in the literature. However, due to particular restrictions on voltage spikes and short circuits, these converters are greatly limited. The operating modes of these converters produce very low switching losses, but the conduction losses are quite large and passive elements carrying large currents must be added.

5.2 Topology Selection

Of the various topologies explained in the previous section, the one chosen for the application specified in Chapter 4 is the Single DAB. Indeed, the low number of switches and passive elements makes this topology one of the most interesting. In addition, the possibility of reducing switching and conduction losses through its control strategy and the opportunity to operate in soft switching conditions make Single DAB the most suitable candidate for the application specified above. This topology can as well ensure the galvanic isolation with its transformer and the bidirectionality.

6
The DAB Converter

In this chapter, the Single DAB converter, which was identified in Chapter 5 as the most suitable topology for the application defined in Chapter 4, is studied. Firstly, a more precise study of its topology and simplified models is carried out (sections 6.2 and 6.3) in order to determine the various components of the converter. Then, a study of the potential losses created by the electronics is carried out in order to carry out the subsequent analyses (section 6.4), and an explanation of what are the switching modes, especially the Zero Volt Switching (ZVS) is (section 6.5). Also, its modulation scheme is defined as well as the different currents flowing through the converter (section 6.6). Once all these elements are known and considered, the dimensioning of the components (section 6.7) and their analyses allow defining the converter fulfilling the objectives announced at the beginning. Finally, an overall analysis (section 6.8) of the converter allows to draw a conclusion on this design and to propose potential improvements that can be carried out.

6.1 Software for this work

The main software used for the analyses and simulation in this work are the followings:

- MatLab Simulink
- PLECS
- Microsoft Office Excel

6.2 Original DAB Converter

A Dual Active Bridge (DAB) converter is composed of two active full bridges circuits made of active gates as semiconductors. They are separated by a high-frequency (HF) transformer and can have in option an additional external inductance. This converter is known to have a high efficiency and a high-power density. It has an ultra-fast dynamic response and the capability of buck-boost operation as well as bidirectional power flow. The figure below shows the circuit schematic of the DAB DCDC converter as it is known.

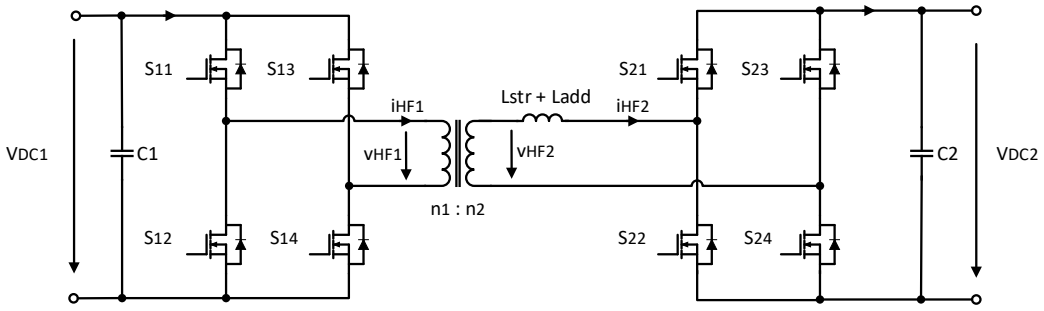

Figure 6.1: DAB Converter circuit

Then the steady-state working principle of the soft-switching DAB converter is explained based on this original circuit implementation, the accompanying modulation scheme and the applied zero voltage switching (ZVS) considerations. In this work case, it is decided to keep the traditional modulation strategy as the phase-shift modulation (PSM), instead of studying all the possible degrees of freedom available for controlling the DAB's active bridges of the converter. This choice is based on the simplicity of its implementation and on its widespread use.

6.3 Lossless DAB Model

Conform to Figure 6.1, the two active bridges implemented as full bridges of active gate-controlled switching devices and anti-parallel freewheeling diode, produce a quasi-square wave voltage as sources $v_{HF1}(t)$ and $v_{HF2}(t)$, which their mean is 0V to not saturate the transformer. Voltage $v_{HF1}(t)$ is equivalent to the DC bus voltage of input, $v_{HF1}(t) = v_{DC1}$, as the voltage $v_{HF2}(t)$ is equal to the DC bus voltage of the output, $v_{HF2}(t) = v_{DC2}$.

Generally, considering an ideal case assuming an infinite magnetizing inductance, relative to the weight of inductance Lm and zero transformer winding resistances as the iron losses Rc and the copper losses R1 and R2, all without any core less, the equivalent circuit of the transformer can be simplified as it is shown in Figure 6.2. The power flow possible to be transferred through the converter is controlled by the current of the stray inductance of the transformer. Frequently, an additional inductance Ladd is added in series to the stray transformer inductance because its critical value for the converter operation is hard to define.

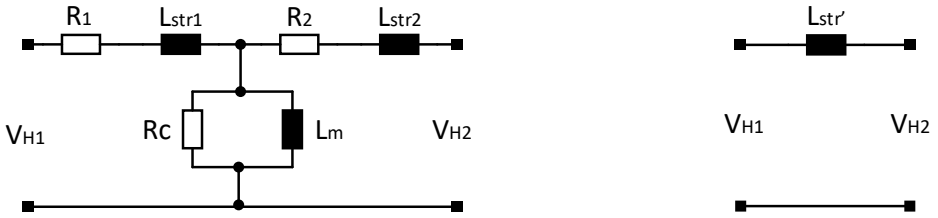

(a) Equivalent transformer circuit (b) Equivalent simplified transformer circuit

Figure 6.2: Transformer circuit simplification

L_{str1} and L_{str2} are corresponding to the leakage inductances of the transformer in each side.

$$L_{str} = L_{str1} + \left(\frac{n_1}{n_2}\right)^2 * L_{str2} + L_{add} \quad (1)$$

Also, to simplify the analysis, the resonant transition duration is significantly shorter than the period of the quasi-square waves, letting to replace the full bridges circuits as input and output by ideal voltage sources v_{HF1} and v'_{HF2}, as shown in Figure 6.3.

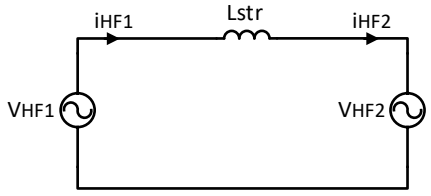

Figure 6.3: Lossless DAB Model

In this configuration, all losses and parasitic elements are neglected. The two ideal voltages sources v_{HF1} and $v_{HF2'}$ are represented from the primary side of the transformer. The relation of v_{HF2} and v'_{HF2} is represented as:

$$v'_{HF2}(t) = \frac{n_1}{n_2} * v_{HF2}(t) \quad (2)$$

The resulting lossless DAB model is depicted in Figure 6.3. Figure 6.6 shows two ways of modulation for the voltages $v_{HF1}(t)$ and $v'_{HF2}(t)$ applied on Lstr. The average DAB DC input current I_{DAB1} or the average DAB DC output current I_{DAB2}, and thus the power energy transfer, are controlled by varying the phase-shift delay (angle = δ) between $v_{HF1}(t)$ and $v'_{HF2}(t)$, as it is explained in the following section. This is the most common way to operate the DAB converter, called the phase-shift modulation (PSM).

6.4 Power losses

In DAB converter different kinds of losses appear based on the topology used. Asa consequence of this, a couple of manners exist to boost its efficiency and can be adopted, in order to reduce them. DAB losses can be categorised as switching losses (P_{SW}), iron losses (P_{IRON}) and ohmic losses (P_{Ohm}). Those two last categories can be grouped as conduction losses (P_{Cond}). Different other losses can appear as in the PCB tracks, copper losses or in DC link capacitors (used for filter). But the highest ones are switching and conduction losses. The modulation strategies' goals are focused on minimizing those losses.

The objective of a high-power density brings the necessity of working in high frequency which increase the size of passive components or reduce the size of transformer. Switching losses has to be minimized most as possible in a high-frequency operation mode.

A big part of this thesis concerns the study of those power losses which brings the choices to do in terms of semiconductors.

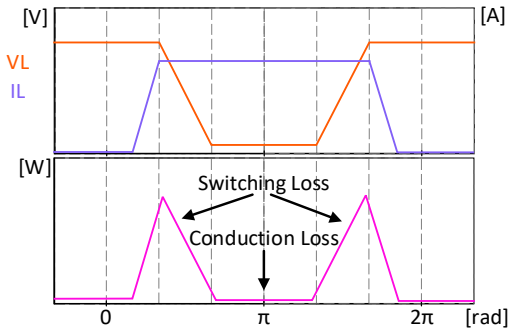

Figure 6.4: Switching losses under hard switching conditions

6.5 Switching modes of semiconductors

The semiconductors in the full bridges of the converter that enable the ripple of the current in the primary and the redress of the current in the secondary can operate in different ways. Those possibilities are presented below.

6.5.1 Hard Switching

Hard switching occurs when a high voltage is applied across the semiconductor as the current increases, see Figure 6.4. The result of this is corresponding to high switching losses. Also, the semiconductor turns off when the current in the collector is high, which also causes losses.

6.5.2 Natural switching

Natural switching is a mode that only concerns uncontrolled semiconductors such as the diode. The losses generated by this switching mode are relatively very low, as a positively polarised diode is considered to have a voltage close to 0 [V].

6.5.3 Soft Switching

The Soft Switching mode reduces switching losses, transformer leakage inductance losses and diode recovery losses. It is possible to classify this mode as ZCS (Zero Current Switching) and ZVS (Zero Voltage Switching). This switching method increases the efficiency of the converter at high frequencies.

6.5.3.1 Zero Current Switching (ZCS)

What is called Zero Current Switching is the way the semiconductor switches when the device current is very low, see Figure 6.5, (a). The turn-on switching takes place when the voltage is almost at zero in order to have the smallest possible overlap, then the current starts to increase. This increasing current is delayed by the action of the parasitic inductance of the transformer. During the turning-off the switching takes place when the current changes direction. The product of the semiconductor voltage and current is low, and therefore the switching losses are also low.

6.5.3.2 Zero Voltage Switching (ZVS)

What is called Zero Voltage Switching is the way the semiconductor switches when the device voltage is very low, see Figure 6.5, (a). Switching takes place when the drain voltage goes to zero during the turn-on phase and then the current in the collector starts to increase. During the turn-off the increase of the drain voltage is slowed down so that it has a minimum overlap with the drain current. Thus, the product of the semiconductor voltage and current is low, and therefore the switching losses are also low.

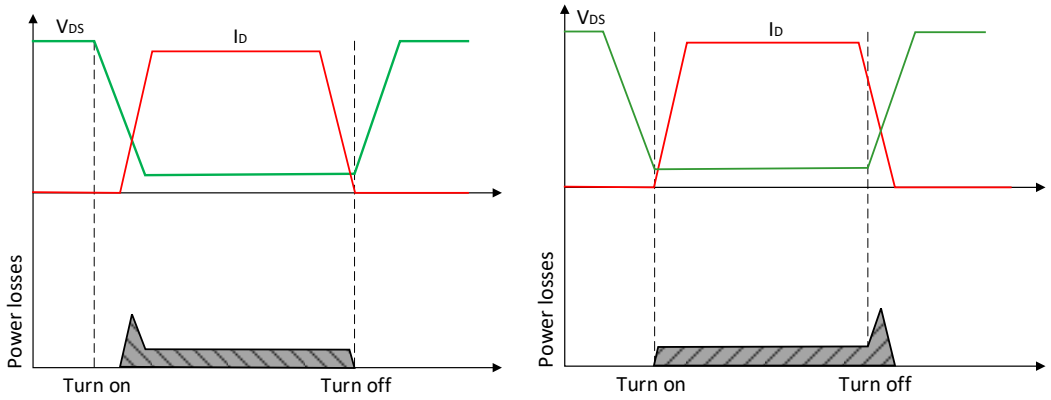

(a) Switching losses under ZCS conditions

(b) Switching losses under ZVS conditions

Figure 6.5: Switching losses under soft switching conditions

6.6 Phase shift modulation

The phase shift modulation (PSM) is the operating process which allows power flow to be transferred through the converter. It exists different phase shifting modulation possible, as the Single-Phase Shift (SPS) modulation, Dual Phase Shift (DPS) modulation and the Triple Phase Shift (TPS) modulation. The differences are due to the possible level of freedom. The SPS modulation is the simplest one, considering it is controlled by one simple shifting angle. Moreover, it is the most spread in the market for converters for its easy control. Nevertheless, it has the least degree of freedom which allow less opportunities to decrease the losses by control. Detailed explanation of the differences and possibilities of each one is addressed on [4].

Although the SPS it does not have the greatest freedom of study, it is the modulation chosen for this work. Considering the goal of this work especially on the analysis of the power devices losses and not on its best modulation scheme generating the least losses possible.

During the SPS modulation, $v_{HF1}(t)$ and $v'_{HF2}(t)$ are modulated with a duty-cycle of 50% (i.e., $\tau 1 = \tau 2 = \pi$ radians (rad)). This means that each voltage source is positive ($v_{HF1} = V_{DC1}$) during a half period ($T_s/2$) and negative ($v_{HF1} = -V_{DC1}$) during the other half one. It is working the same on the other side. The switching period is defined as $T_s = 2\pi$.

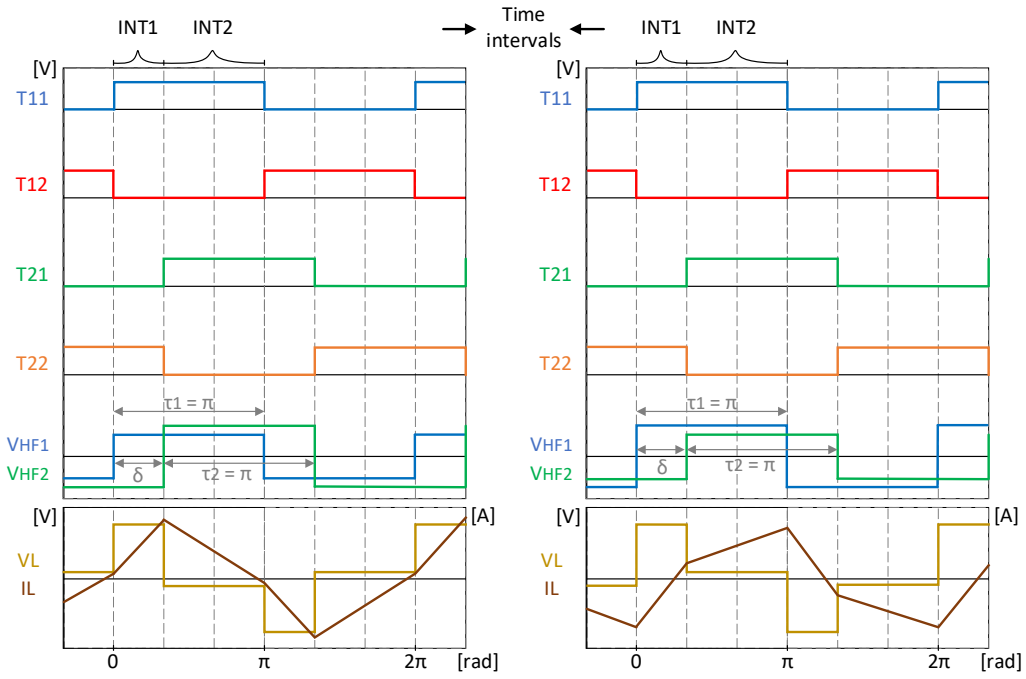

Figure 6.6: SPS modulations

a) SPS modulation mode positive power flow Hard switching operation

b) SPS modulation mode negative power flow Soft switching operation

Single Phase Shift modulation means, as it is said in its name, a single shift with a single angle. There are different possibilities depending on the angle, see Figure 6.6, presented as example here below:

(a)	Mode 1+	δ >= 0	Positive power flow
(b)	Mode 1-	δ <= 0	Negative power flow

As it is shown in the Figure 6.6, these two modes are acting differently on the current which is passing through the inductance. It is important to know that the condition when there is the maximum power transferred through the converter is when the angle δ is the half of the half period, i.e., $T_s/4$.

Also, the waveforms showing the signal is periodic during the half of period, if we take in account it is inverted during the second half period. Therefore, it is possible to size the

converter by getting focused on the half period. According to the Figure 6.6, two main time intervals are interesting:

INT1:	$st_{leg11} = 1$ {s_{11} on, s_{12} off}	$st_{leg11} = 0$ {s_{13} off, s_{14} on}
	$st_{leg21} = 0$ {s_{21} off, s_{22} on}	$st_{leg21} = 1$ {s_{23} on, s_{24} off}
INT2:	$st_{leg11} = 1$ {s_{11} on, s_{12} off}	$st_{leg11} = 0$ {s_{13} off, s_{14} on}
	$st_{leg21} = 1$ {s_{21} on, s_{22} off}	$st_{leg21} = 0$ {s_{23} off, s_{24} on}

Table 3: State of switching devices during INT1 and INT2

The inductances from the transformer being unknown, even usually it is rare that constructors give these values in datasheet, it is interesting to understand what total inductance L_{str} is necessary for this converter with the specifications given in Chapter 4. As well, understanding how work the converter with this modulation scheme and what are the results depending on different variables.

6.6.1 Equations of Inductor Current, Angle and Power transfer

In a previous time, it is important to understand the different voltage sources, and also the inductor voltage and the inductor current are repeating every half-cycle in changing their signs. According to the time intervals it has been shown previously, it is possible to define the current passing through the inductance, seen from one bridge as:

$0 < \vartheta < \delta$:

$$i_{L_{1str}} = i_L(\delta) = i_L(0) + \frac{\frac{n_1}{n_2} * V_{DC1} + V_{DC2}}{\omega L}\vartheta \qquad (3)$$

$\delta < \vartheta < \pi$:

$$i_{L_{1str}} = -i_L(0) = -\left(i_L(\delta) + \frac{\frac{n_1}{n_2} * V_{DC1} - V_{DC2}}{\omega L}(\vartheta - \delta) \right) \qquad (4)$$

$$i_L(0) = \frac{\frac{n_1}{n_2} * V_{DC1}(d(\pi - 2\delta) + \pi)}{2\omega L} \qquad (5)$$

$$i_L(\delta) = \frac{\frac{n_1}{n_2} * V_{DC1}(2\delta - \pi + d\pi)}{2\omega L} \qquad (6)$$

With this current knowledge it is possible to describe the power equation which define the parameter necessary for the sizing of this converter. The expression of the power is known as:

$$P = f(\delta) = \int_0^{\pi} \frac{1}{\pi} V_{HF} I_{HF} \qquad (7)$$

After transformations including the equations of the different variables, the result of the expression is given like:

$$P_{B1} = \frac{\frac{n_1}{n_2} * V_{DC1}}{Ts} \int_{kTs}^{(k+1)Ts} i_1(t)dt \tag{8}$$

$$= \frac{\frac{n_1}{n_2} * V_{DC1}}{Ts} \left(\begin{array}{l} \int_0^{\delta} \left(\frac{\frac{n_1}{n_2} * V_{DC1} + V_{DC2}}{\omega L} \vartheta + \frac{\frac{n_1}{n_2} * V_{DC1}(d(\pi - 2\delta) + \pi)}{2\omega L} \right) d\vartheta + \\ \int_{\delta}^{\pi} \left(\frac{\frac{n_1}{n_2} * V_{DC1} - V_{DC2}}{\omega L} (\vartheta - \delta) + \frac{\frac{n_1}{n_2} * V_{DC1}(2\delta - \pi + d\pi)}{2\omega L} \right) d\vartheta \end{array} \right)$$

Or in P.U:

$$P_{B1_{P.U.}} = \frac{\frac{n_1}{n_2}}{Ts} \int_{\frac{kTs}{\pi}}^{\left(\frac{k+1}{\pi}\right)Ts} i_1(t)dt \tag{9}$$

$$= \frac{\frac{n_1}{n_2}}{Ts} \left(\int_0^{\frac{\delta}{\pi}} \left(\left(\frac{n_1}{n_2} + d\right) \vartheta + \frac{\frac{n_1}{n_2} * (d(\pi - 2\delta) + \pi)}{2} \right) d\vartheta + \int_{\frac{\delta}{\pi}}^{1} \left(\left(\frac{n_1}{n_2} - d\right) (\vartheta - \delta) + \frac{\frac{n_1}{n_2} * (2\delta - \pi + d\pi)}{2} \right) d\vartheta \right)$$

From this expression it is possible to isolate the δ to understand how the angle works for a specific power:

$$\delta = \frac{\pi \left(V_{DC2} n_2 + 2\sqrt{\left(\frac{{V_{DC1}}^2 d^2 {n_1}^2}{2} - \frac{V_{DC1} V_{DC2} d n_1 n_2}{2} + \frac{{V_{DC2}}^2 {n_2}^2}{4} - 2 f_{sw} L P_{B1} d n_1 n_2\right.\right.}}{2 V_{DC1} d n_1} \tag{10}$$

Or in P.U:

$$\delta_{P.U.} = \frac{\pi \left(d n_2 + \sqrt{-\frac{d * (4 P n_1 n_2 - 2\pi d {n_1}^2 - \pi d {n_2}^2 + 2\pi d n_1 n_2)}{\pi}}\right.}{2 d n_1} \tag{11}$$

The power can be expressed from the second bridge as well. The conditions of the two-time intervals must be taken in consideration, because for the second one the sign changes in the first part of the equation:

$$P_{B2_{P.U.}} = \frac{\frac{n_1}{n_2} * d}{Ts} \left(\begin{array}{l} \int_0^{\frac{\delta}{\pi}} - \left(\left(\frac{n_1}{n_2} + d\right) \vartheta + \frac{\frac{n_1}{n_2} * (d(\pi - 2\delta) + \pi)}{2} \right) d\vartheta \\ + \int_{\frac{\delta}{\pi}}^{1} \left(\left(\frac{n_1}{n_2} - d\right) (\vartheta - \delta) + \frac{\frac{n_1}{n_2} * (2\delta - \pi + d\pi)}{2} \right) d\vartheta \end{array} \right) \tag{12}$$

In a second hand, the current passing through the inductance can be evaluated as:

$$I_{Lstr_{rms}} = \sqrt{\frac{1}{\pi} \int_0^{\pi} \left(I_L(\vartheta)\right)^2 d\vartheta} = \sqrt{\frac{1}{\pi} \left(\int_0^{\delta} {i_{L1}}_{INT_1} d\vartheta + \int_{\delta}^{\pi} {i_{L1}}_{INT_2} d\vartheta \right)} \tag{13}$$

$$I_{Lstr_{rms}} = \sqrt{\frac{1}{\pi} \left(\begin{array}{l} \int_0^{\delta} \left(\frac{\frac{n_1}{n_2} * V_{DC1} + V_{DC2}}{\omega L} \vartheta + \frac{\frac{n_1}{n_2} * V_{DC1}(d(\pi - 2\delta) + \pi)}{2\omega L} \right) d\vartheta \\ + \int_{\delta}^{\pi} \left(\frac{\frac{n_1}{n_2} * V_{DC1} - V_{DC2}}{\omega L} (\vartheta - \delta) + \frac{\frac{n_1}{n_2} * V_{DC1}(2\delta - \pi + d\pi)}{2\omega L} \right) d\vartheta \end{array} \right)}$$

These equations allow to set up the converter as wanted in defining some variables and then control if the results correspond to what it is calculated. From those equation it is possible to understand that the angle giving the maximum power transfer possible is at $T_s/4$ which that it corresponds to:

$$\delta = 2\pi/4 \ = \ 1{,}57\ [\text{rad}] \quad \text{or} \quad 0{,}5\ [\text{p.u.}]$$

With this angle it is possible to define the value of the necessary total inductance L_{str} by taking the transformed equation of power viewed from the first bridge:

$$L_{str} = \frac{V_{DC1}n_1\left(\frac{\delta^2\left(\frac{V_{DC1}n_1}{n_2}+V_{DC2}\right)}{4\pi f_{sw}} - \frac{\left(\delta V_{DC1}n_1(\pi-\delta(\pi-2\delta))\right)}{4\pi f_{sw}n_2} + \frac{((\pi-\delta)(V_{DC1}n_1-\pi V_{DC2}n_2+\delta V_{DC2}n_2+\pi\delta V_{DC1}n_1))}{4\pi f_{sw}n_2}\right)}{\pi P_{B1}n_2} \tag{14}$$

The value of the inductance considering the 20% of power added for security is given as:

$$L_{str} = 74{,}93\ [\mu H]$$

In the meantime, the value of RMS current through the inductance is given as:

$$I_{Lstr_{rms}} = 40{,}21\ A$$

6.6.2 Modulation waveforms analysis

In modelling the converter on software, it is possible to see the waveforms of the current $I_{Lstr}(t)$ and the voltages $v_{HF1}(t)$ and $v'_{HF2}(t)$ to analyse if the theory matches with reality.

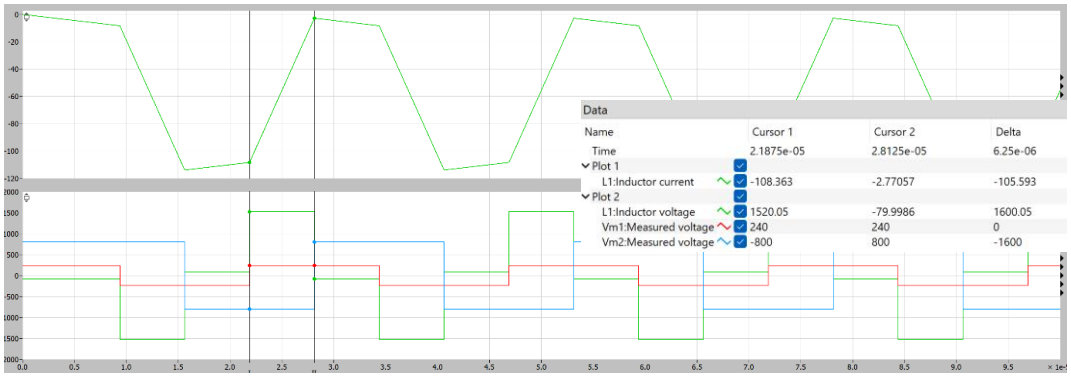

Figure 6.7: Waveforms from the converter sized for the specific application

In this case, the power without the additional 20% is setting to see what should be expected in a real waveform on the converter. The signal captured is looking like expected for the application.

6.7 Sizing of components

Once the operating mode and the situation in which the converter has to operate are known, the components can be sized. In this part, the aim is to find the components that generate the least possible losses and that are the most efficient. In addition, first it is question of finding components on the market that can be used in the well-known application of the converter, and then analysing their behaviour (section 6.7.1). Component analysis consist in grouping components that do the necessary work and ensuring that they generate the least possible losses. Most of the losses are thermal. This is why an overall thermal analysis of the system is important to design the equipment so that it produces as little heat as possible and dissipates it as much as possible (section 6.7.2). Finally, a discussion of the choice of the component is made to ensure the analysis (section 6.7.3).

6.7.1 Necessary components

Several components are needed to build this DAB converter. Semiconductors are used for the two bridges. A transformer is needed to provide the required galvanic isolation. Passive elements must also be dimensioned to make the converter filters. Then, elements allowing the evaluation of losses such as heatsinks, and fans are essential to the converter. The study of the control electronics of the semiconductors is not part of this thesis, but it is necessary to dedicate some space to it. Furthermore, the surface area required by the latter is relatively small, which has little influence on the final volume of the converter.

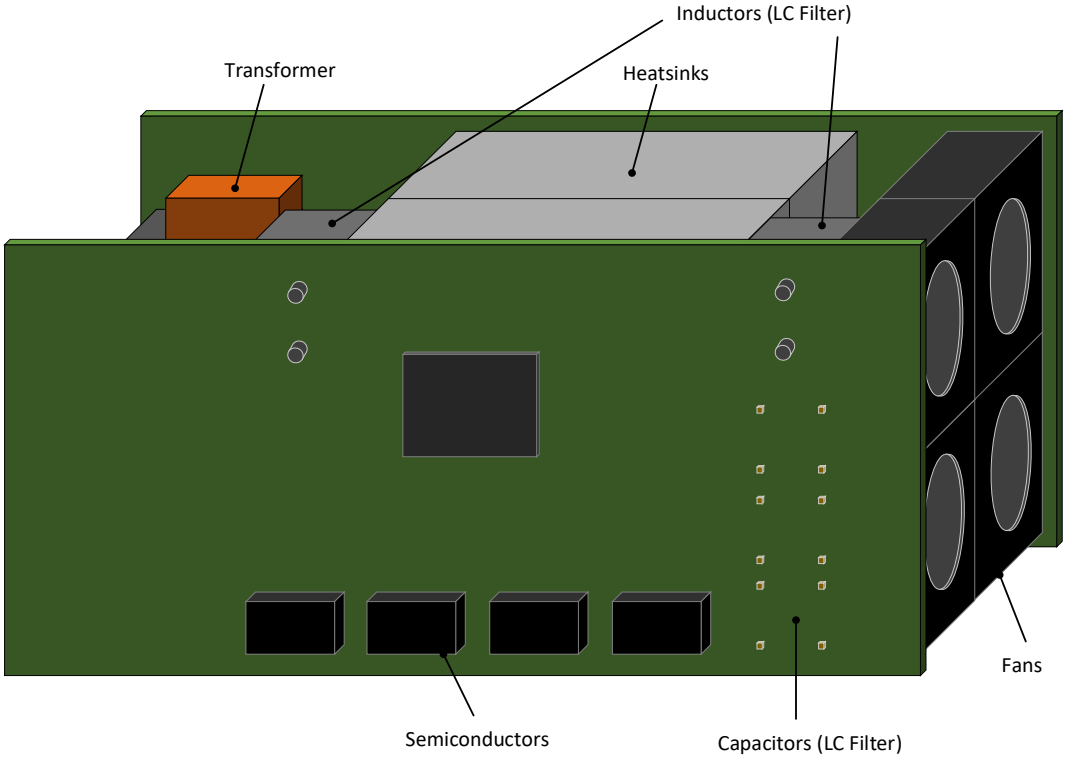

Figure 6.8: 3D schematic of the converter

The following sections describe the methods for sizing the components. For reasons of initial specification, the sizing of radiators and fans is done first.

6.7.1.1 Heatsinks and Fans

As stated in the description of the application, the mechanical part of the heatsinks and fans are based on projects that have already been carried out with satisfactory results for these elements. Therefore, the suppliers and starting characteristics of these components are known:

Object	**Brand**	**Model**	**Specification**
Heatsink	Guasch	RG42080L24/110RM	Length = 110mm Fins = 24
Fan	Sanyo Denki	9G0824G101	Parallel

Table 4: Heatsinks and Fans manufacturer choice

Knowing the models of the components, the objective of the design is to find the thermal resistance values for them. These data are necessary for the correct modelling of the converter for the loss analysis. It is important to mention that it is desired that the fans are positioned in parallel, in order to have a higher air flow. Also, two heatsinks are to be provided, one under each full semiconductor bridge.

The goal of sizing the fans and the heatsink which will allow to evacuate the thermal losses produced by the semiconductors, is to combine them to see the thermal resistance it is possible to get and then analyse it to define if the heat evacuation is sufficient. With the specification curves given in the datasheet, it is possible to compare them to get the thermal resistance (R_{thH-A}).

6.7.1.1.1 Sizing of Heatsinks and Fans

Firstly, the characteristic curves given by the radiator manufacturer should be noted, Figure 6.9. The Heat Sink Specific Heat curve is given in [Pa] and the Heat Sink Density curve is given in [K/W], which correspond to thermal resistance values [22][23].

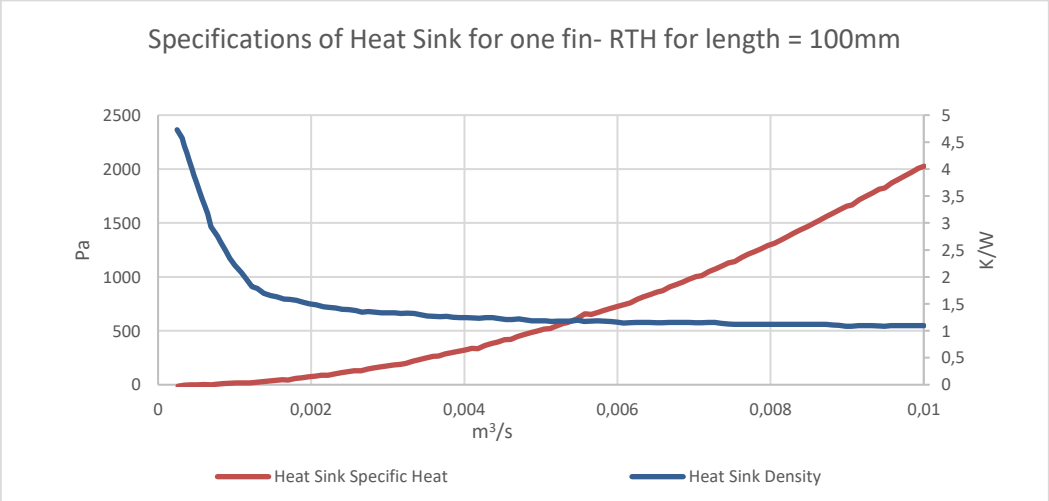

Figure 6.9: Specifications of heatsink

Next, the characteristic curve in [Pa] for one fan should also be recorded, Figure 6.10. From this curve it is possible to deduce the curve for the use of two fans. Indeed, depending on the position of them, the result is not the same. Two fans in series give a higher pressure,

while two fans in parallel give a higher airflow. The latter is required in order to have a larger air volume to cool the radiators.

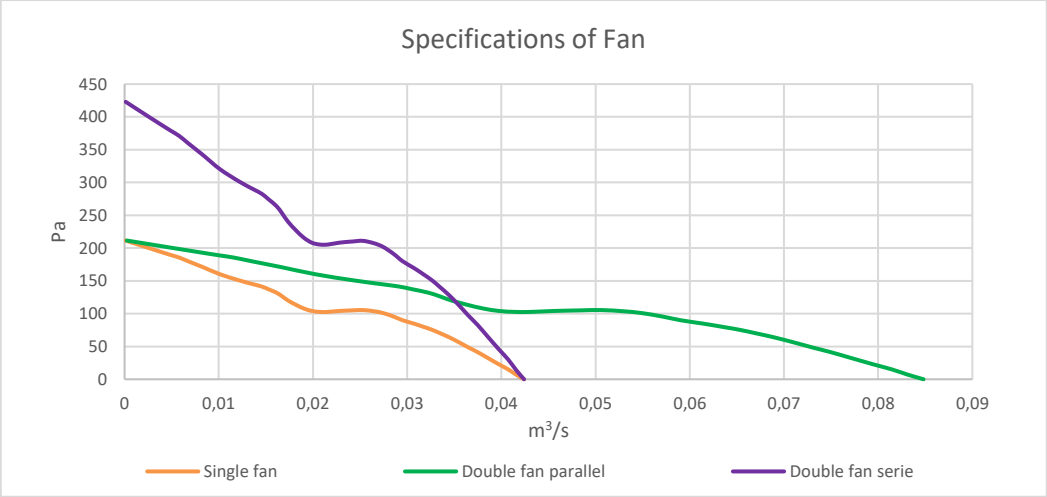

Figure 6.10: Specifications of fan

The objective is to obtain the thermal resistance value resulting from the fan/radiator combination. To find this value, the curves must be superimposed in order to compare them. Where the curves for Heatsink Specific Heat and Double Fan Parallel intersect, this is the pressure value for the simultaneous use of both elements. This pressure is equal to approximately 336 [Pa] for an air flow of 0,00325 [m3/s]. It is then possible to define the thermal resistance value for this given air flow. Moving up the Heat Sink Density curve, the thermal resistance value is given as 1,32 [K/W] when using both components.

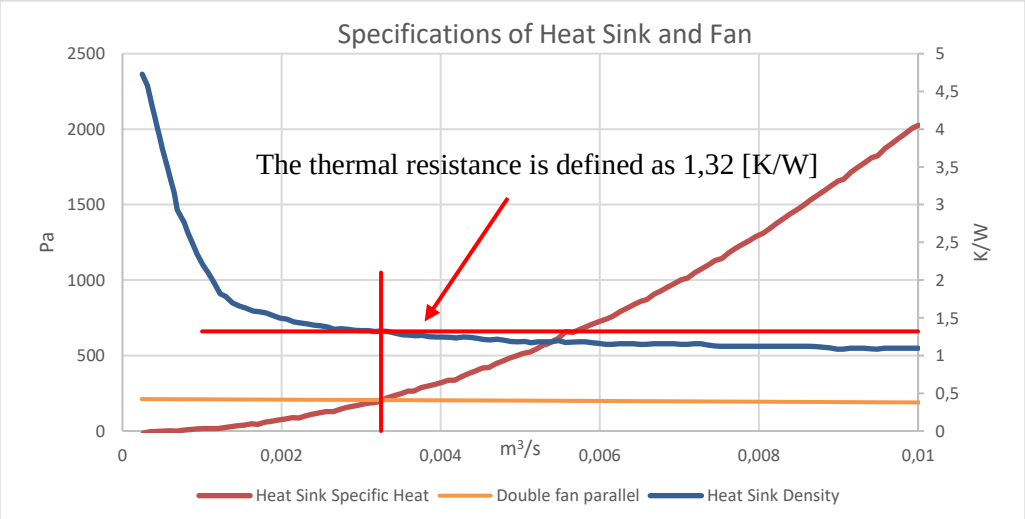

Figure 6.11: Specifications graphs of fans and heatsink necessary to evacuate the heat of the semiconductor

However, it is important to note that this thermal resistance value is only suitable for one radiator fin. Depending on the supplier, the value for one fin should be divided by the number of fins in the radiator.

$$Rth_{H-A} = \frac{Rth_{fin}}{n_{fins}} \tag{14}$$

The number of fins is available in the model's name: RG42080L**24**/110RM, i.e., 24 fins for this type of radiator. The final thermal resistance of the radiator when using two fans in parallel is defined as follows:

$$Rth_{H-A} = \frac{1{,}32}{24} = 0{,}055 \left[\frac{K}{W}\right] \quad (15)$$

This thermal resistance should therefore be considered in the converter model for the overall thermal analysis of the converter.

6.7.1.2 Semiconductors

The choice of semiconductors is important, because for a specific application some are more suitable than others. That is why the study of different components corresponding to certain basic characteristics that match with the converter must be simulated in order to retain only those that allow an optimal application.

Knowing the current semiconductor market, which is in crisis, it is necessary to be able to find good components at not too exorbitant prices and especially that are in stock or can be delivered in a not too long time. These criteria have become essential in the development of all power electronic equipment. The dependence on the US for semiconductor design and China for production, which are not on good terms at the moment, makes Europe vulnerable in terms of its competitiveness in the electronics market. Nevertheless, Europe is waking up and starting to fund more and more the semiconductor development and production market, which heralds a brighter future for the research of new technologies dependent on this sector.

6.7.1.2.1 Sizing of the semiconductors

The sizing of the semiconductors for this converter synchronises market products with the application in which the converter is to be used. Firstly, research is carried out to find a range of semiconductors that match the characteristics required of them. These choices are made according to the criteria described below. Once several components have been selected, they are analysed, and the choice is made at the end when all the data can be compared.

The semiconductors required for the design of this converter are MOSFETs with antiparallel DIODES. In order to integrate them into the system, they must be able to meet the following characteristics and choices:

Primary

Package	**Vds [V]**	**Ids [A]**
TO-247	240 + (30%) = 312	83,33

Secondary

Package	**Vds [V]**	**Ids [A]**
TO-247	800 + (30%) = 1040	25

The following criteria depend on what is available on the market (data base July 2022). As said before, the choice is very limited. In order to choose for each bridge which semiconductors are suitable, a selection of several available MOSFETs is made to analyse them and thus determine which ones are suitable for this converter [7] to [15].

The preselection is made on the basis of:

- Possible DC current in the drain
- Possible power dissipation
- Turn-On switching losses
- Turn-Off switching losses
- Available stock
- Factory turnaround time
- Price per unit

These first criteria allow to see the capabilities of each selected semiconductor and to compare them with each other. Depending on the availability of the market, which was extremely variable throughout the thesis, three semiconductors were selected for Bridge 1 and six for Bridge 2, see Table 5.

	Brand - Model	Technology	Vds [V]	Id [A]	Rds(on) [mΩ]
First Bridge	Microchip - MSC015SMA070B	SiC	700	140	19
	Infineon - IPW60R017C7XKSA1	Si	600	109	17
	IXYS - IXTK120N65X2	Si	650	120	23
Second Bridge	ONSEMI - NTHL020N120SC1	SiC	1200	103	28
	Wolfspeed - C3M0016120D	SiC	1200	115	22,3
	Microchip - MSC017SMA120B	SiC	1200	113	22
	Wolfspeed - C3M0021120D	SiC	1200	100	28,8
	Microchip - MSC025SMA120B	SiC	1200	103	31
	UnitedSiC - UF3SC120016K3S	SiC	1200	107	21

Table 5: Semiconductors preselection

According to the criteria mentioned above, it is possible to compare them and to get a first idea of which semiconductors are the most complete in all aspects. In the following charts, the maximum values in each category are based on all manufacturer data and therefore on maximum values that can be reached for some semiconductors. The percentage scales are therefore intended for comparison between semiconductors and not to define values for the whole market.

6.7.1.2.1.1 First Bridge Preselection

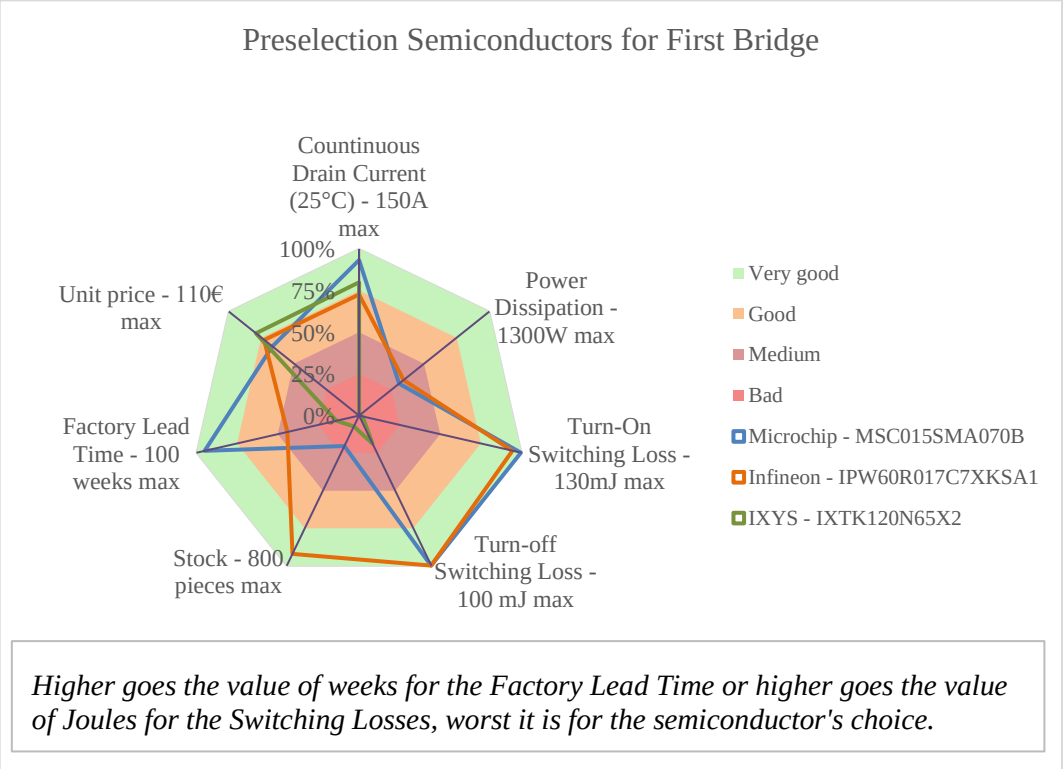

Figure 6.12: Radar graphic for preselection of semiconductors in first bridge

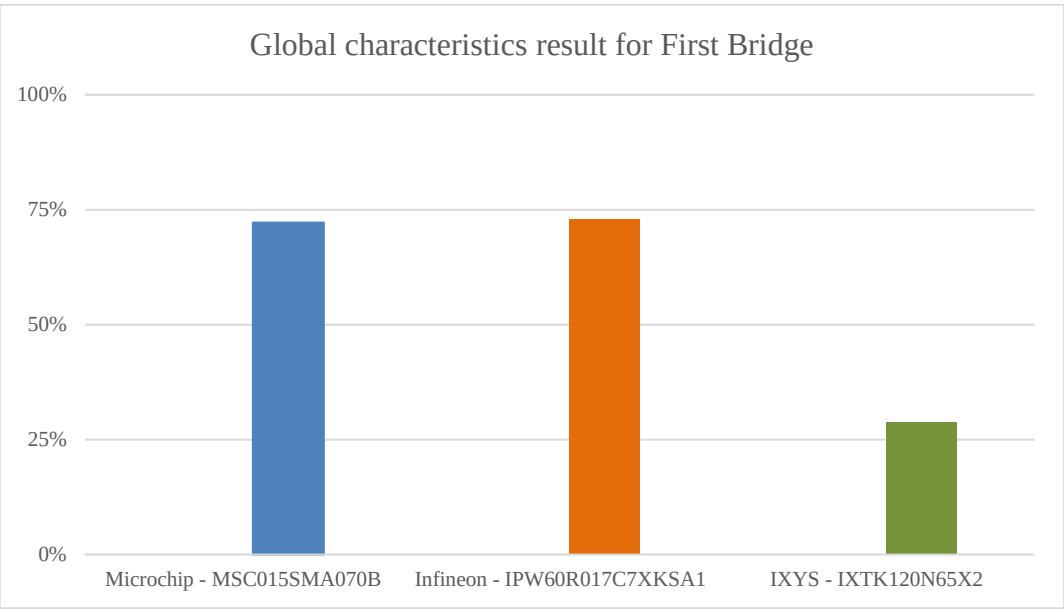

Figure 6.13: Global characteristics result for the semiconductor preselection of the first bridge

For the first bridge, these three semiconductors were selected and compared with their own characteristics. The first two obviously have more interesting characteristics. Although the one designed by Microchip is equipped with SiC technology, which is more recent than the one of Infineon, their electronic characteristics are relatively similar at first sight. The differences lie in the logistical basis of the suppliers, who have different stocks and lead times.

6.7.1.2.1.2 Second Bridge Preselection

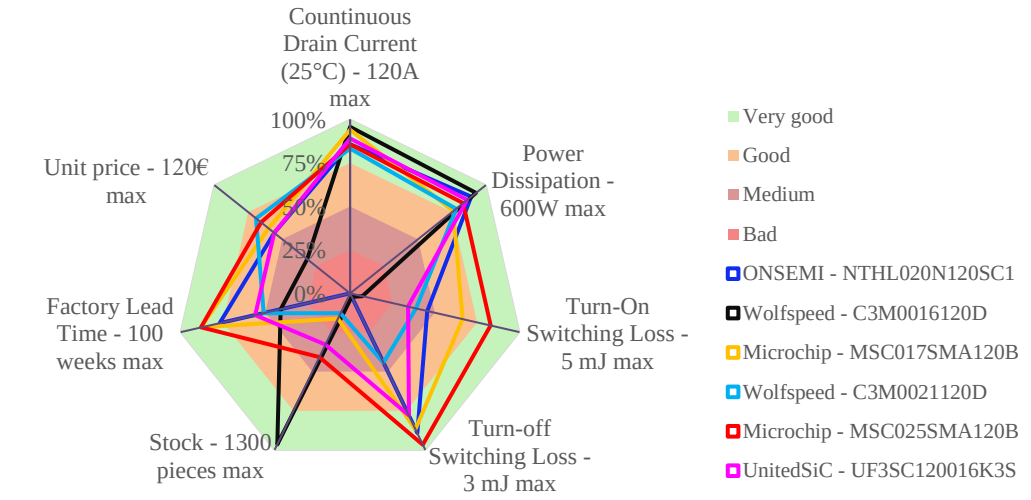

Higher goes the value of weeks for the Factory Lead Time or higher goes the value of Joules for the Switching Losses, worst it is for the semiconductor's choice.

Figure 6.14: Radar graphic for preselection of semiconductors in second bridge

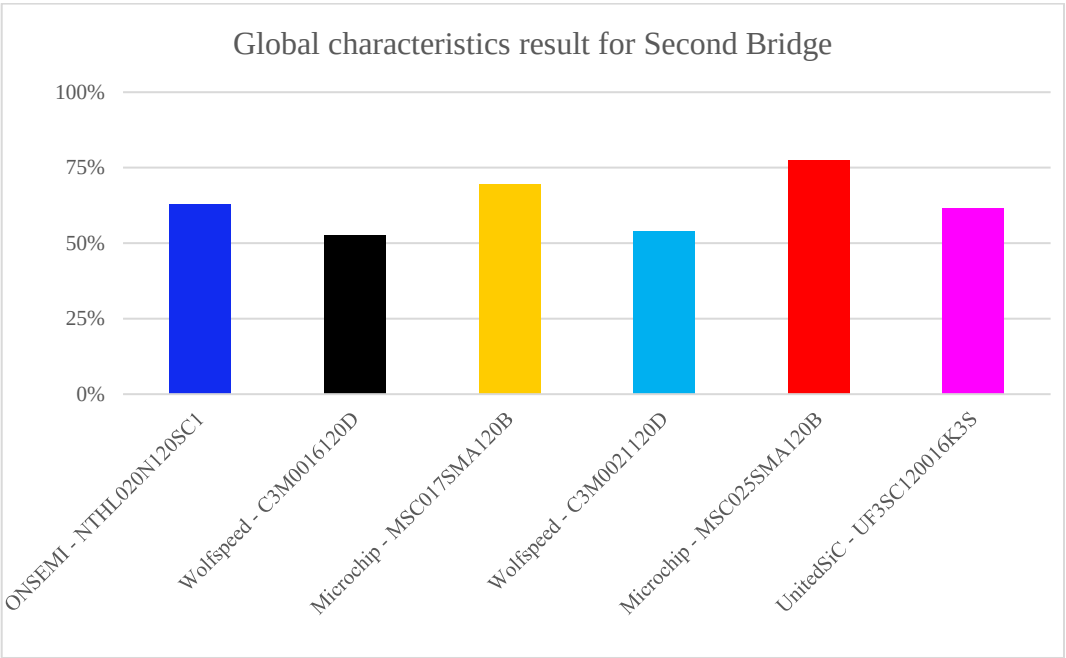

Figure 6.15: Global characteristics result for the semiconductor preselection of the second bridge

For the second bridge, these six semiconductors were selected and also compared with their own characteristics. It seems that all of them are more or less equal in terms of possible DC current in the drain, power dissipation and turn-off switching losses. The differences appear especially in the Turn-On switching losses and the logistic part, which differs for each supplier.

On this first analysis, some components can be defined as more suitable for the converter. However, what is important is that the semiconductors are able to produce the required function, but above all with as little loss as possible. For this reason, the thermal analysis for each preselected model is imperative to determine which ones can be considered for the converter.

6.7.1.3 Insulator

The insulator is a necessary element because the metallized part of the semiconductor in contact with the heatsink is polarized with the positive voltage of the MOSFET. To not electrify the heatsink, which would cause a problem, an insulator film must be glued between the components, allowing only the heat flow to pass through but electrically isolating the two parts. In order to be able to thermally analyse the model with all the components, it is important to be able to dimension this film and especially its thermal resistance, which must be integrated into the thermal model.

6.7.1.3.1 Sizing of the insulator

The choice of insulator is based on existing products on the market [17]. The Bergquist Company offers such a product. The data for the insulator film is given for a semiconductor model with a TO-220 packageTo find its thermal resistance, it is necessary to adapt these data for the semiconductor model of the converter, i.e., with the "TO-247" package. Only the dimensions change between these two models and thus the surface area. The film thickness remains the same.

TO-220 (50 psi)

Surf. Max.	0,263 [in2]	**Surf. Min.**	0,242 [in2]
TO-220 Thermal Perf. [°C/W] 0,0010''			0,92
Thermal Impedance [°C-in2/W]			0,12

TO-247 (50 psi)

Surf. Max.	0,501 [in2]	**Surf. Min.**	0,466 [in2]
TO-220 Thermal Perf. [°C/W] 0,0010''			0,48
Thermal Impedance [°C-in2/W]			0,12

Table 6: Insulators specifications depending on the package

According to the supplier's data, the thermal resistance for the "TO-247" package can be deduced as below. This data must then be included in the thermal analysis.

$$Rth_{C-H} = 0{,}48 \left[\frac{K}{W}\right] \tag{16}$$

6.7.1.4 LC Filter

The objective in developing a converter, although its application is defined, is that it can adapt to the network in which it is placed. This is why, not knowing if this network is very disturbed, a converter is equipped by default with upstream and downstream filters guaranteeing a clean signal in the conversion unit.

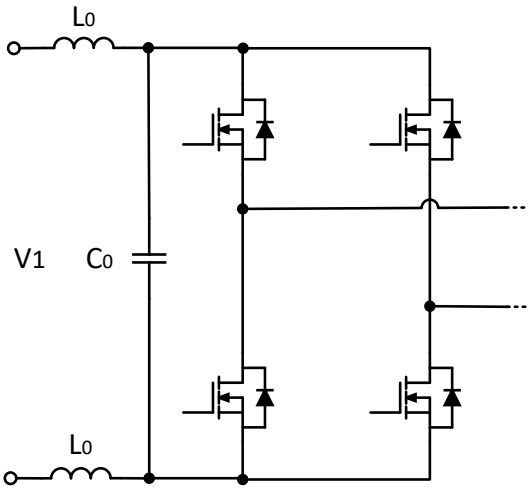

Figure 6.16: Added filter on primary side (IN)

Two inductances with the value of L_0 are sized as one inductance total L and one capacitor C_0 are the necessary components.

6.7.1.4.1 Sizing of LC filter

Thus, LC filters are sized to match the converter via the second order transfer function as follows:

$$G_p(s) = \frac{I_{OUT}}{I_C} = \frac{1}{LCs^2 + 1} \tag{17}$$

Since the inverter operates at a frequency of 40 [kHz], the current on the DC In and Out buses ripples at twice the frequency, i.e., 80 [kHz].

$$|G_p|_{f \to 80kHz} = \frac{1}{|LC(jw)^2 + 1|} \tag{18}$$

On the input bus, connected to the battery, the current is about 170 [A]. In order to limit the current on the battery, an attenuation of 100x is recommended and thus a charge/discharge current of 1,7 [A].

$$\frac{I_{OUT}}{I_C} = 0{,}01 \tag{19}$$

To size the two components of the filter, it is necessary to define one of the two and then find the value of the second. For this application with high currents, there are few choices of inductances. Therefore, these are defined first. The supplier "VISHAY" produces inductances that can evolve under high current constraints. The choice of inductances (paralleled for each bus) [18][19], knowing that the current value at the output bus is about 60 [A], is defined as follows:

BUS	BUS'es current [A]	Heat Rating Current DC Typ. [A]	L0 INDUCT. [µH]	L INDUCT. TOTAL [µH]
IN	167,80	154,00	0,68	1,34
OUT	55,90	96,00	3,30	6,60

Table 7: Initial inductances choice

The capacitors can therefore be defined according to the inductances that have been chosen.

$$\frac{I_{OUT}}{I_C} = \frac{1}{|L_{choosed} C(2\pi 80kHz)^2 + 1|} \rightarrow C = \frac{\frac{I_C}{I_{OUT}} - 1}{4 * L_{choosed} * (80kHz)^2 * \pi^2} \quad (20)$$

BUS	C0 CAPACITOR [nF]
IN	292,40
OUT	59,40

Table 8: Initial capacitors choice

With the values of capacitors defined above, a software simulation can be realized, in order to ensure the attenuation is made correctly. The waveforms compared before and after the filter in both bridges are represented below :

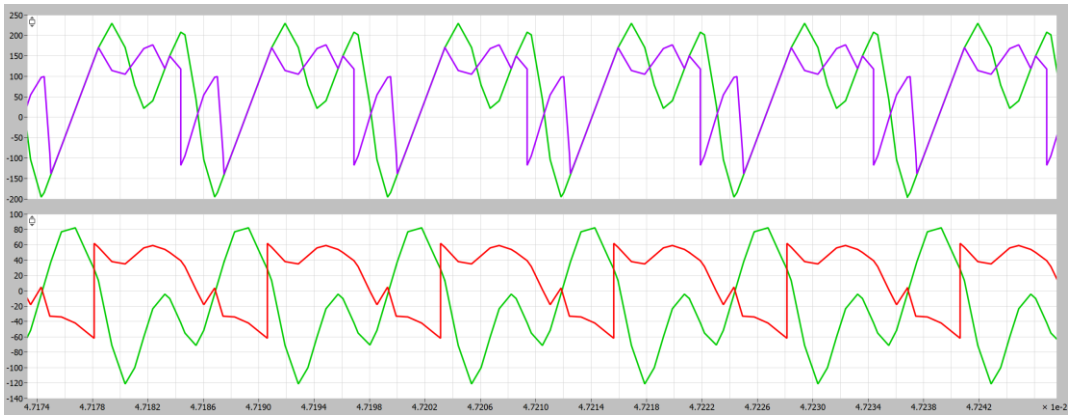

Figure 6.17: Comparison of waveforms before and after the filer

The result of the simulation shows a problem of resonance with the values of the capacitors chosen before. The filter does not work as it should be. To understand what is happening, the transfer function is represented in a bode diagram, see Figure 6.18, to demonstrate the cause of this issue.

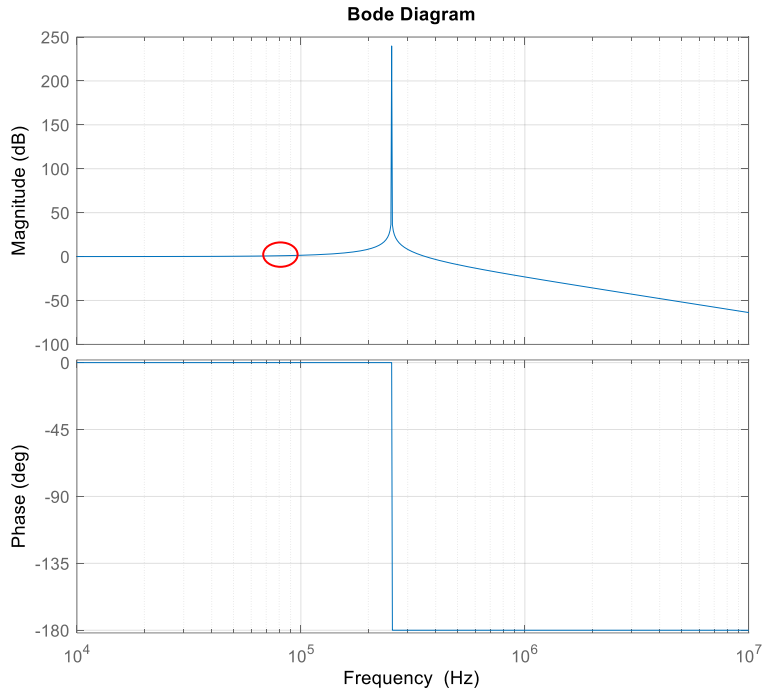

Figure 6.18: Bode diagram of transfer function of the filter in primary side (IN)

Indeed, for some frequencies, there is a possibility the filter plays a role of excitement instead of attenuation. In the case of the sizing of this filter, a frequency of 80 [kHz] is used. This frequency, firstly, is situated on the let of the resonant peak, which means it is not attenuated. Secondly, the multiple of this frequency, as harmonics, can be situated in the peak, which is the case at the frequency 240 [kHz]. This is the reason why the filter makes an opposite effect of what it has to do.

Considering, the inductances fixed, the value of the capacitor has to been increased, to move the frequency used on the right of the resonant peak, to ensure the filter does not excite the system.

To have an attenuation of 100x the filter as to be at -40 [dB] at 80 [kHz]. After some tries, the new values of the capacitors are given as:

BUS	C0 CAPACITOR [µF]
IN	295,00
OUT	60,00

Table 9: Choice of capacitors for attenuation of 100x

These values give new bode diagrams which guarantees the filter effect on the system.

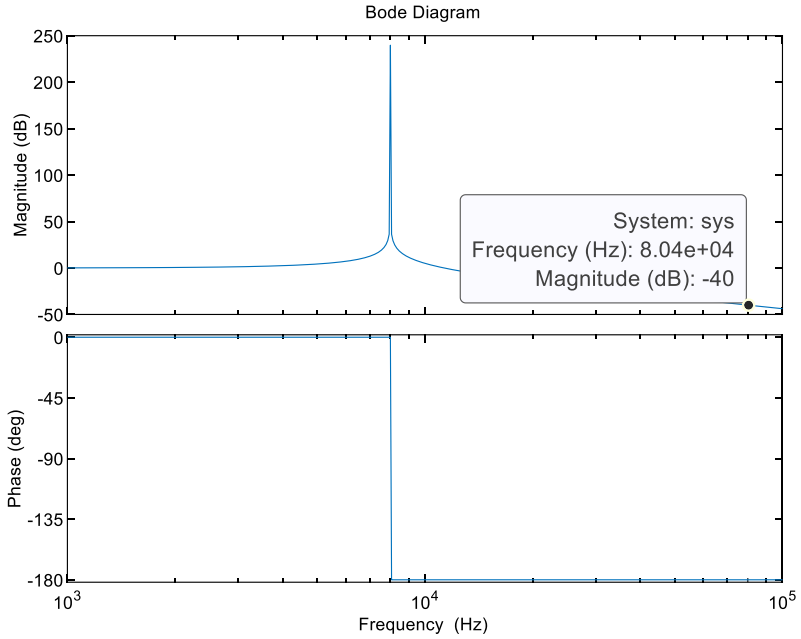

Figure 6.19: Bode diagram of transfer function of the filter in primary side with new value of capacitor

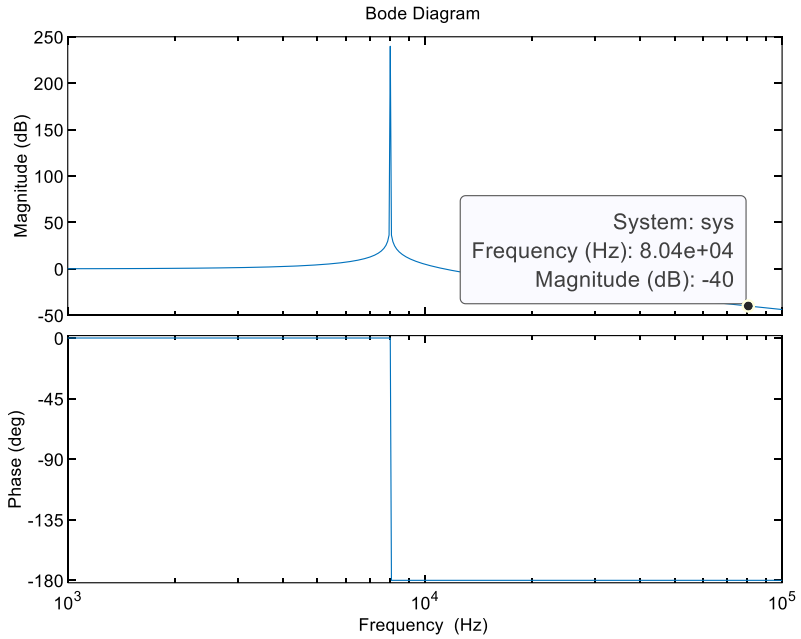

Figure 6.20: Bode diagram of transfer function of filter in secondary side (OUT) with new value of capacitor

However, depending on the mechanical part already defined by the existing project this thesis is based on [ref], the place available for the capacitors is reduced. The components chosen for this application are explained in the choice section 6.7.3.4 based on this previous study.

6.7.1.5 Transformer

The transformer is referred on the project described formerly. It is necessary for the galvanic isolation. Its stray inductance has been explained in previous section and its ratio is equal

to 3:1. No more information about its sizing are given in this work, some information is available in [3].

6.7.2 Thermal Analysis

The purpose of the thermal analysis is to observe the power losses emitted by the electronic components that dissipate as heat through the whole converter. This helps to determine whether the choice of components is correct and to ensure that such a converter does not destroy itself when put into operation.

This thermal analysis is performed with the PLECS modelling tool.

6.7.2.1 Analogy between thermal and electrical systems

An analogy is possible to be made between thermal and electrical systems [24]. Each layer composing the assembly of the semiconductor on its heat evacuation components can be represented by a resistor. The goal is to do an analysis of the thermal behaviour of the electronic of the converter to see if the sizing of the component evacuates enough heat. By doing it in this way, the heat is represented by the current (Q = i), the temperature at one point as the voltage (T = V) and the conduction resistance as an electrical resistor (Θ or R_{th} = R).

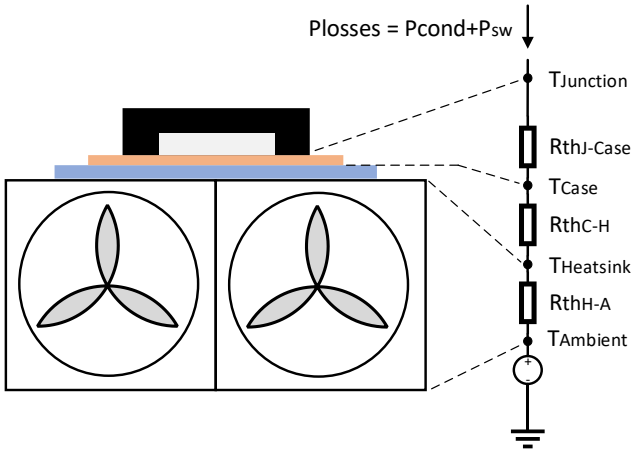

Figure 6.21: Thermal analogy with electrical system

6.7.2.2 Structure of the model

The structure below, represent the thermal resistances for each component of one bridge. The simulation is based on this structure for the analysis.

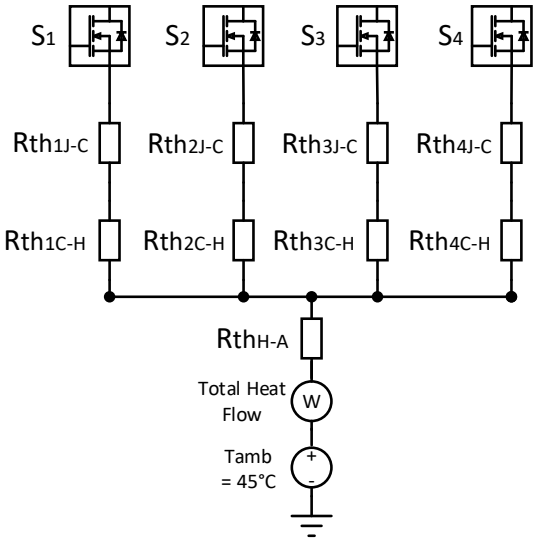

Figure 6.22: Structure of one bridge for thermal analysis

Switching and conduction losses are created by the semiconductors and are dissipated in the different thermal resistance of junction, insulator, and heatsink/fans.

6.7.2.3 Settings of the semiconductors

The thermal analysis of semiconductors is important because it allows to justify or not the trends of the pre-selection made before. To analyse these elements, it is necessary to be able to model various important concepts :

- Turn-On Switching Losses
- Turn-Off Switching Losses
- Conduction Losses

These three parameters are an integral part of the semiconductor and must be modelled for the MOSFET and for the DIODE component. These data come directly from the suppliers' datasheets. On the other hand, the switching loss parameters can be defined in two ways, by equations or by graphical data provided by the manufacturer [7] to [15]. Turn-On Switching Losses parameter for MOSFET.

Graphic

The Turn-On Switching Losses can be defined graphically from the manufacturer's datasheet and their values can be integrated into a lookup table for modelling the component.

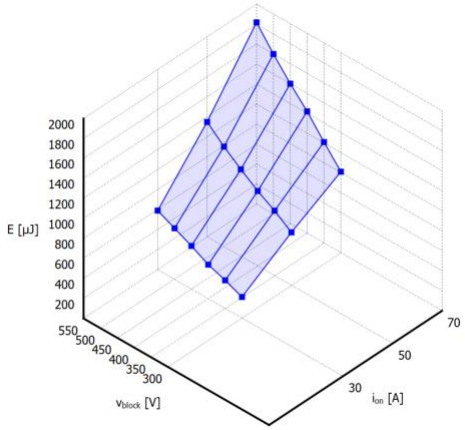

Figure 6.23 : Graphic of Turn-On Switching Losses lookup table for the semiconductor « Microchip – MSC015SMA070B »

Equation

The second possibility is to use an equation that approximates the switching losses [16]. This method is still based on data provided by the datasheet.

$$E_{on} \cong \frac{V_{dc} I_{out}}{2} \left(\frac{Q_{GS2} + Q_{GD}}{V_{drv} - V_{GSpl}} R_{g,tot} \right) + V_{dc} Q_{rr} \tag{21}$$

6.7.2.3.1 Turn-Off Switching Losses parameter for MOSFET

Graphic

Turn-Off Switching Losses can also be defined graphically from the manufacturer's datasheet.

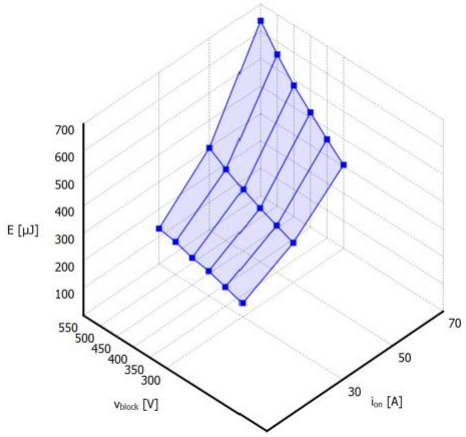

Figure 6.24 : Graphic of Turn-Off Switching Losses lookup table for the semiconductor « Microchip – MSC015SMA070B »

Equation

The equation for Turn-Off Switching Losses is defined as follows:

$$E_{off} \cong \frac{V_{dc} I_{out}}{2} \left(\frac{Q_{GS2} + Q_{GD}}{V_{drv} - V_{GSpl}} R_{g,tot} \right) \tag{22}$$

It is important to note that suppliers only provide data for semiconductors with SiC technology. The use of the equation is therefore mandatory for the modelling of Si technology components.

6.7.2.3.2 Turn-Off Switching Losses parameter for DIODE

For the diode, only the Turn-Off Switching Losses are considered for its modelling. These can only be represented by an equation given as :

$$E_{rr} \cong \frac{V_{dc} Q_{rr}}{4} \tag{23}$$

The values of the variables can be found in the component datasheet.

6.7.2.3.3 Conduction Losses parameter for MOSFET

Graphic

Conduction losses are the last losses to be modelled for each component. The data concerning them are available in the manufacturers' datasheets. They can be integrated graphically into a lookup table as for switching losses. They are available for all technologies, whether SiC or Si.

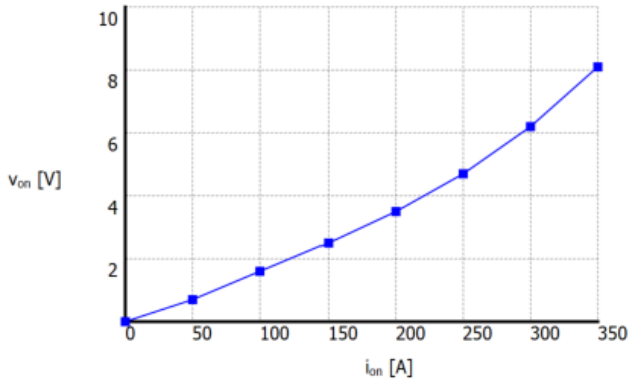

Figure 6.25: Graphic of Conduction Losses lookup table for the MOSFET « Microchip – MSC015SMA070B »

Equation

They can also be defined with the following equation:

$$P_{cond} = V_{Q0} I_{Q,avg} + R_Q I^2{}_{Q,rms} \tag{24}$$

Since the value of V_{Q0} is equal to 0 [V] for a current of 0 [A], see Figure 6.25, the equation can be simplified as :

$$P_{cond} = R_Q I^2{}_{Q,rms} \tag{25}$$

For reasons of accuracy, when graphical data is available from the manufacturers, this method is chosen to model the components.

6.7.2.3.4 Conduction Losses parameter for DIODE

In the same way as for the MOSFET, the conduction losses for the DIODE can be graphically integrated into a lookup table.

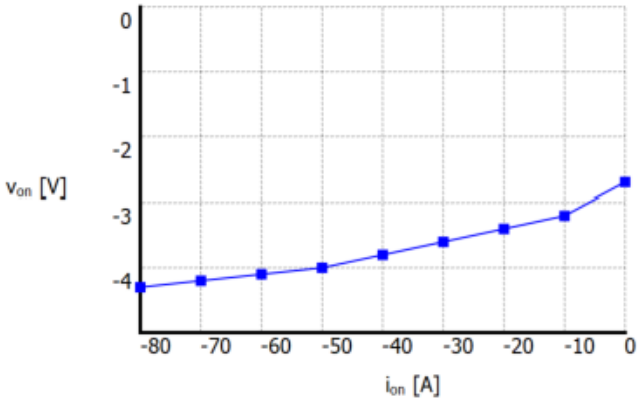

Figure 6.26: Graphic of Conduction Losses lookup table for the DIODE « Microchip – MSC015SMA070B »

They can be defined by the same equation as for the MOSFET. Since V_{Q0} is not equal to 0 [V] for a current of 0 [A], see Figure 6.26, the full equation can be used.

6.7.2.4 Analysis of the semiconductors of the selection

The analysis of the selected semiconductors is carried out according to the structure presented above, but is performed several times, to cover all the components of the selection. It is done for each semiconductor in order to be able to compare them in the same way as the pre-selection was done. In order to ensure safety for the sizing and knowing that the environment in which the components evolve is hot, the ambient test temperature is raised to 45°C. This allows a margin of choice to be made in selecting semiconductors that are certain to work for the specified application.

This analysis is based on different results that must be compared to define the ideal components. These results correspond to measurement points such as:

- Semiconductor's junction temperature
- Heatsink's temperature
- MOSFET's conduction losses
- DIODE's conduction losses
- MOSFET's switching losses
- DIODE's switching losses
- Heat flow through the converter

These measurements allow the clear identification of the semiconductor and thus the possibility to compare it with others. It is important to note that the heatsink should not exceed 65 [°C] and the semiconductor units should not exceed 100 [°C].

As with the pre-selection of components, the following graphs are also made with qualitative percentage scales. This is for comparative purposes only and has nothing to do with the quality of the components, which in some cases may be more suitable for other applications. All the measures are available in the Appendix A.

6.7.2.4.1 Measurement of the First Bridge

For the first bridge, the three pre-selected semiconductors are modelled according to their datasheet to be measured in the thermal structure of the converter. As said before, the components with "Si" technology cannot be modelled graphically due to lack of information from the manufacturers. Two of the three possible components for the first bridge are made with this technology and therefore the analysis is done with equation modelling.

The first set of measurements gives the following data:

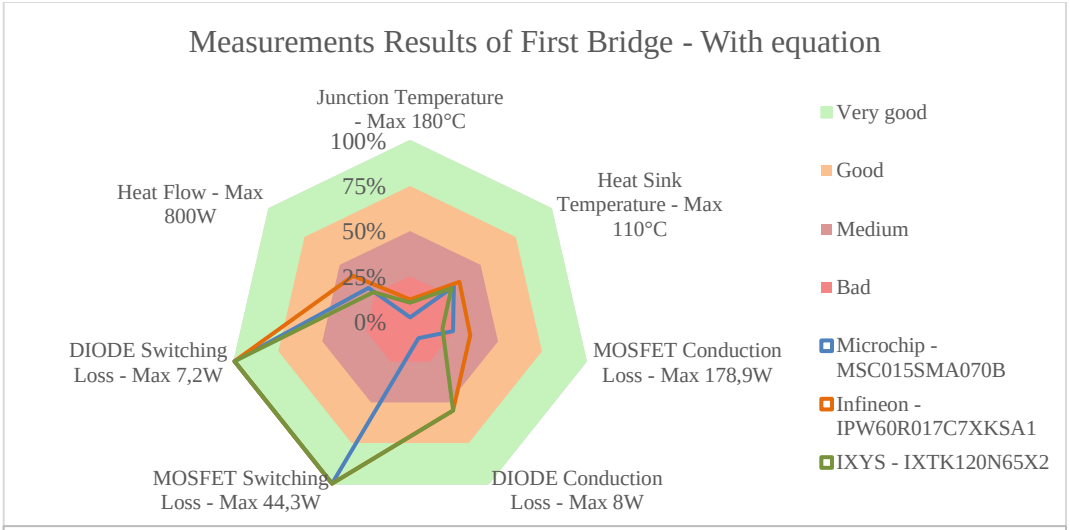

Higher are the values of these parameters, worse it is for the converter. This is why the max. value presented are equal to 0% and lower the values are, closer to 100% they go.

Figure 6.27: Radar graphic of measurements results of first bridge with equation's method

The table below shows the junction temperatures for a unit and the radiator which are represented on the radar graph above.

	Microchip - MSC015SMA070B	Infineon - IPW60R017C7XKSA1	IXYS - IXTK120N65X2
Junction Temperature [°C]	176,20	158,30	161,30
Heat Sink Temperature [°C]	75,90	71,50	77,70

Table 10: Temperatures measured on the first bridge with equation's method

It is clear that the assembly with these components in this analysis is really not good and the safety temperatures are not respected at all. A modification of the assembly must be made to use these components. In order to reduce the losses through the power devices, one possibility is to create a bridge with semiconductors in parallel. This allows the current on each element to be divided and reduces the power losses. The diagram below shows the necessary arrangement:

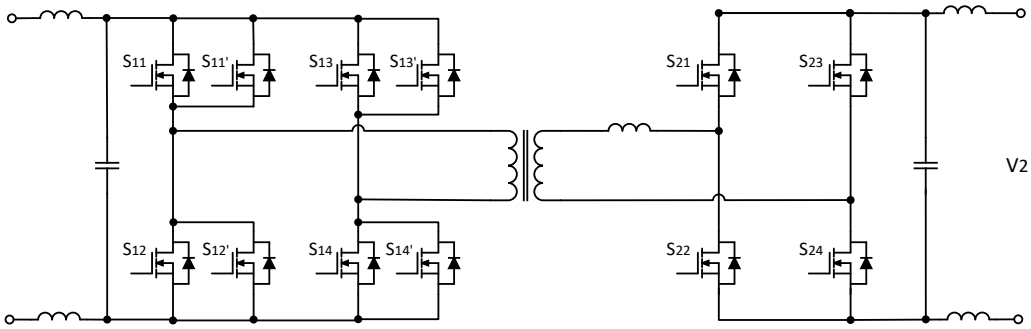

Figure 6.28: Final DAB circuit with first bridge including power devices in parallel

A second analysis is then performed with the new bridge assembly and the series of measurements gives the following data:

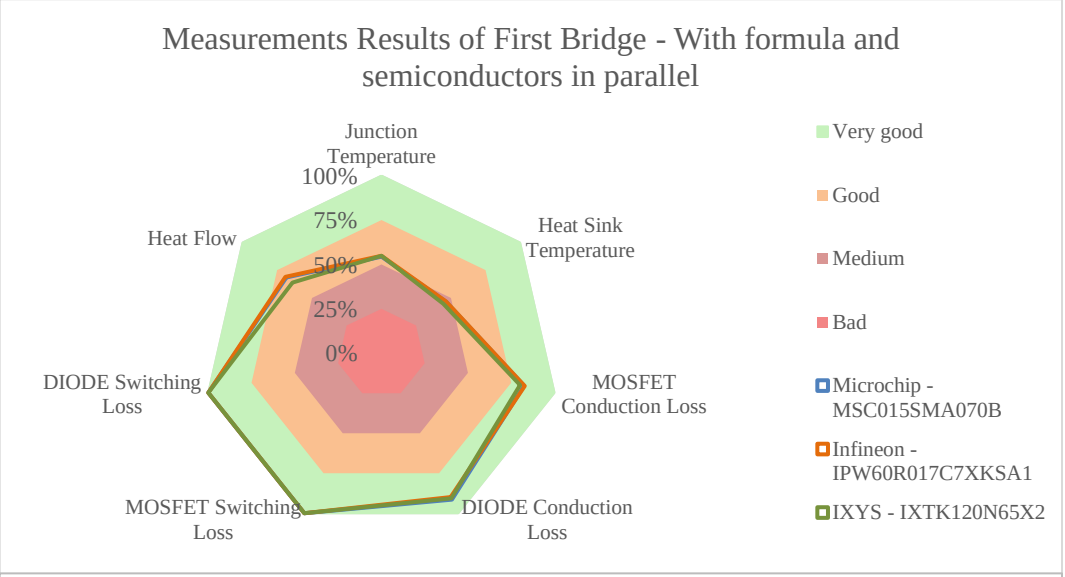

Higher are the values of these parameters, worse it is for the converter. This is why the max. value presented are equal to 0% and lower the values are, closer to 100% they go.

Figure 6.29: Radar graphic of measurements results of first bridge with equation's method and semiconductors in parallel

	Microchip - MSC015SMA070B	**Infineon - IPW60R017C7XKSA1**	**IXYS - IXTK120N65X2**
Junction Temperature [°C]	82,10	81,20	81,20
Heat Sink Temperature [°C]	58,80	58,60	60,90

Table 11: Temperatures measured on the first bridge with equation method and semiconductors in parallel

The change to the bridge assembly shows a radical change in the measurements. The safety temperatures are respected and the results for each semiconductor are much better. Clearly, the three semiconductors are quite equal, and this data can be used for the final choice of components.

A last series of measurements can be done on this first bridge concerning the semiconductor of the manufacturer "Microchip". Indeed, being made with the "SiC" technology, the possibility of measuring its graphic model can be interesting.

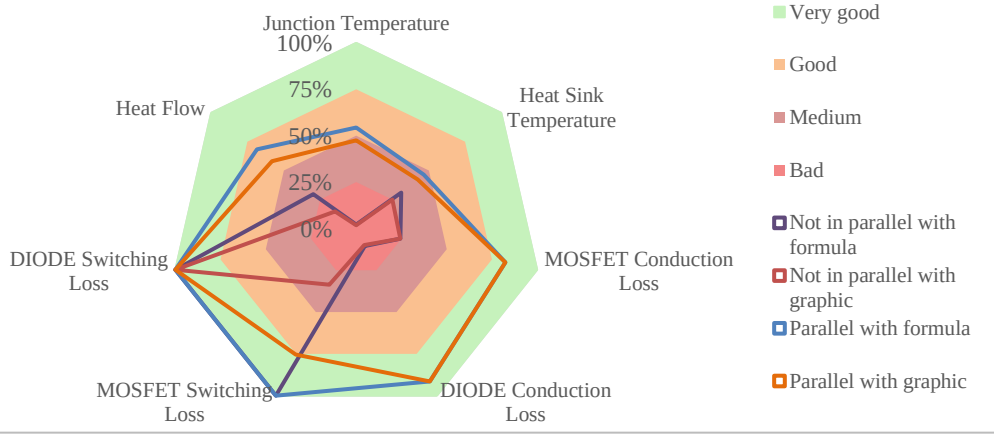

Higher are the values of these parameters, worse it is for the converter. This is why the max. value presented are equal to 0% and lower the values are, closer to 100% they go.

Figure 6.30: Radar graphic of measurements results of Microchip - MSC015SMA070B in different cases

	Not in parallel with formula	**Not in parallel with graphic**	**Parallel with formula**	**Parallel with graphic**
Junction Temperature [°C]	176,20	176,90	82,10	94,55
Heat Sink Temperature [°C]	75,90	82,60	58,80	63,50

Table 12: Temperatures measured on Microchip - MSC015SMA070B in different cases

By comparing the first component with its different modelling possibilities, a first observation can be made. The change to parallel connection really improves the temperatures. Secondly, the equation might tend to be light on the switching losses on the MOSFET. The reality of the manufacturer's measurements gives fewer good values for this notion. Nevertheless, this concept is not verifiable with the other two components. The choice of the appropriate semiconductor for this first bridge must then be made in consideration of the elements of the preselection.

6.7.2.4.2 Measurement of the Second Bridge

For the first bridge, the three pre-selected semiconductors are modelized according to their datasheet in order to be measured in the thermal structure of the converter. As said before, the components with "Si" technology cannot be modelized graphically due to lack of information from the manufacturers. Two of the three possible components for the first bridge are made with this technology and therefore the analysis is done with equation modelling.

For the second bridge, the six semiconductors of the preselection are also modelized from their datasheet and then measured according to the established thermal structure. On the other hand, as they are all made of "SiC" technology, for which the manufacturers provide the parameters concerning switching losses, they are modelled first with the equation, then graphically. This process allows the two methods to be compared and conclusions to be drawn.

The first series of measurements with the selection of semiconductors modelled by equation gives the following data:

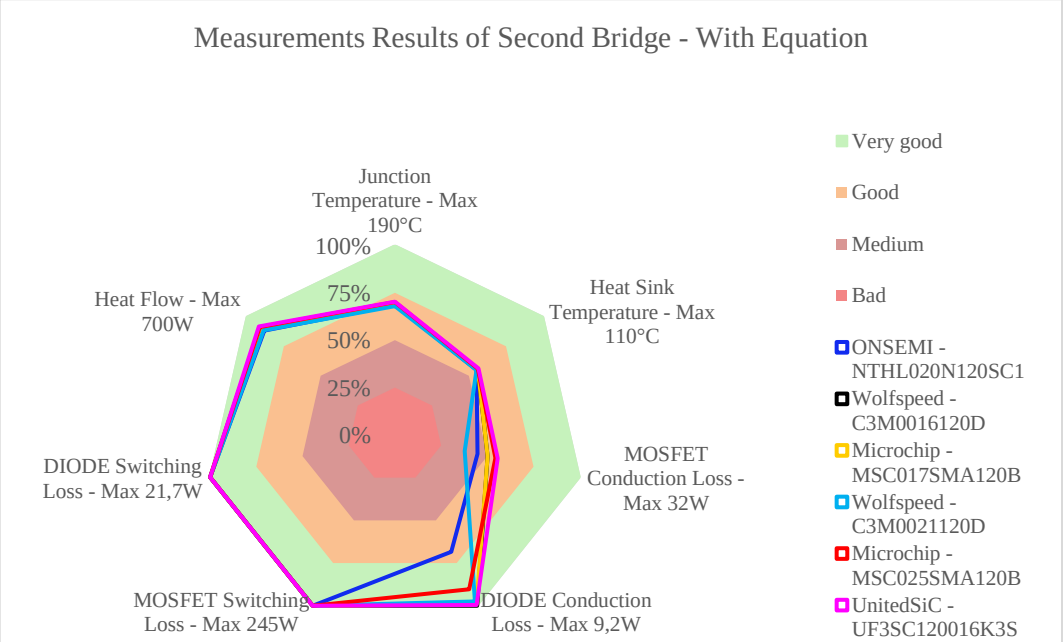

Higher are the values of these parameters, worse it is for the converter. This is why the max. value presented are equal to 0% and lower the values are, closer to 100% they go.

Figure 6.31: Radar graphic of measurements results of second bridge with equation's method

The graph above shows that the different components are relatively similar. The notable differences are in the modelling of the conduction losses, which are visibly worse for the semiconductor of the manufacturer "ONSEMI" and the second one of "Wolfspeed". The test measurements with the second modelling method can be interesting to be analysed to compare the different components.

The second series of measurements is made with the graphic modelling of the components for their losses and gives the following comparison results:

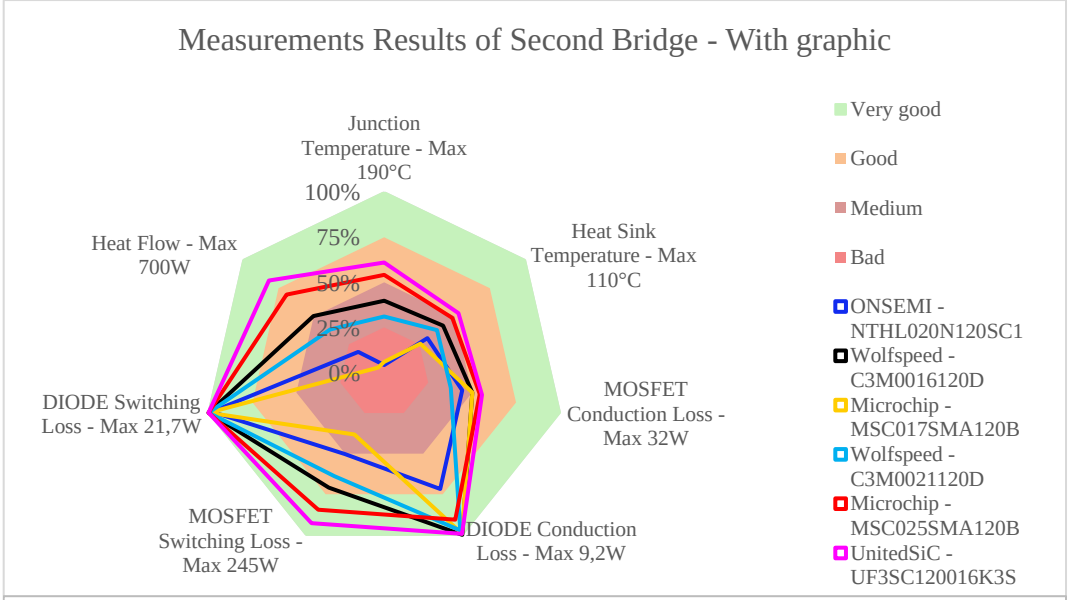

Higher are the values of these parameters, worse it is for the converter. This is why the max. value presented are equal to 0% and lower the values are, closer to 100% they go.

Figure 6.32: Radar graphic of measurements results of second bridge with graphic's method

This series shows more diverse differences between the individual semiconductors than the previous method. The device from the manufacturer "UnitedSic" maintains its values rather well with both methods. In contrast, the other devices have worse results with the second method. Also, two important points are that all components below 50% for the junction temperature, are above 95 [°C], and those below 50% for the heatsink temperature, are above 60 [°C]. These differences are highlighted when deciding on the components and the favourable method will be defined for the final choice.

6.7.3 Choice of the components

The choice of components is based on the studies realised in the previous sections. Some of the components are already defined from the start and have been used to size the other elements needed for the converter.

6.7.3.1 Heatsink

As described above, the radiator is already defined from the beginning. It is the model "RG42080L24/110RM" from the supplier "Guasch". In the case of this converter, one heatsinks per bridge is required. Therefore, two similar heatsinks are required to build the converter. The price for this model of heatsink is 63,00 [€] which means a total of 126,00 [€].

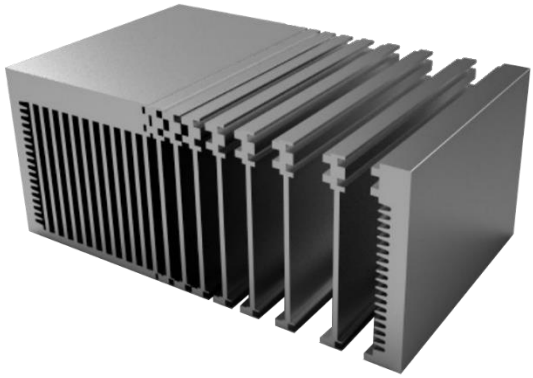

Figure 6.33: Picture of potential heatsink from Guash used on the converter

6.7.3.2 Fans

The fans are also defined from the start. This is the "9G0824G101" model from the supplier "Sanyo Denki". They are placed in parallel after a heat sink. This means that two fans are required for each heat sink, making a total of four for the inverter. The unit price of this fan is around 28,00 [€] which means a total of 122,00 [€].

Figure 6.34: Picture of fans from Sanyo Denko used on the converter

The interesting thing about their location is that if the transformer and other elements are placed on the opposite side, they also receive the air flow and can be cooled.

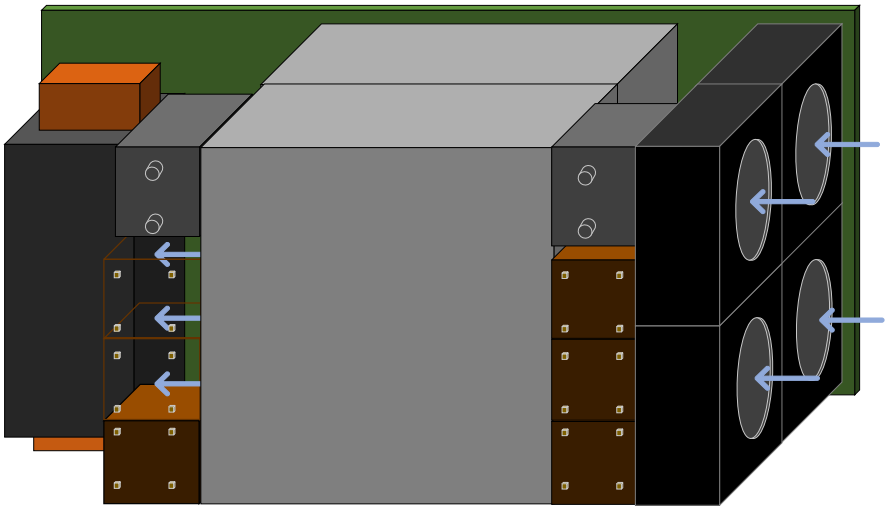

Figure 6.35: Air flow passing through the converter

The blue arrows showed on the Figure 6.35, represent the air flow created by fans which crossed the converter. All the components are not studied to be refreshed, but this mechanical environment allowing this way for the air flow is based on the project [3].

6.7.3.3 Choice of the insulator

The choice of insulator has already been made in the sizing part of its thermal resistor. It is based on one product of the manufacturer "Berguist" who provide this type of insulator film [17]. The cost of this product, useful for more than one semiconductor is around 115,00 [€].

Figure 6.36: Image of the insulator film from Berguist

6.7.3.4 Choice of the component for the LC filter

The necessary components for the LC filter have been described in the section 6.7.1.4. The inductances [18][19] for these two filters have been fixed at the beginning and correspond to :

BUS	Brand	Model	L0 IND. [µH]	Unit price [€]
IN	Vishay	IHXL1500VZEBR68M5A	2 x 0,68 = 1,34	32,86
OUT	Vishay	IHXL1500VZEB3R3M5A	2 x 3,30 = 6,60	33,63

Table 13: Inductances manufacturer for LC filter

Figure 6.37: Inductance type from Vishay manufacturer for the LC filter

The capacitors have sized for the attenuation wanted. But as it has been said, the place available in the converter mechanic for the capacitors is reduced. Based on [3] the space presented let the place for a maximum of six capacitors with the package measurements maximum as 43 [mm] x 21,5 [mm].

After research of components available on market, which accept the limit of voltage for both bridges as 300 [V] for the first one and 900 [V] for the second one, with the maximum capacitance possible in order to attenuate the most possible the current, the selected ones are:

BUS	Brand	Model	C0 CAPA. [µF]	Unit price [€]
IN	Kyocera AVX	FFB54H0276KJC	6 x 27 = 162	15,80
OUT	Vishay	MKP1848612094P4	6 x 12 = 72	11,83

Table 14: Capacitors manufacturers for LC filter

The bode diagrams given with these new values are represented below, Figure 6.38 and Figure 6.39:

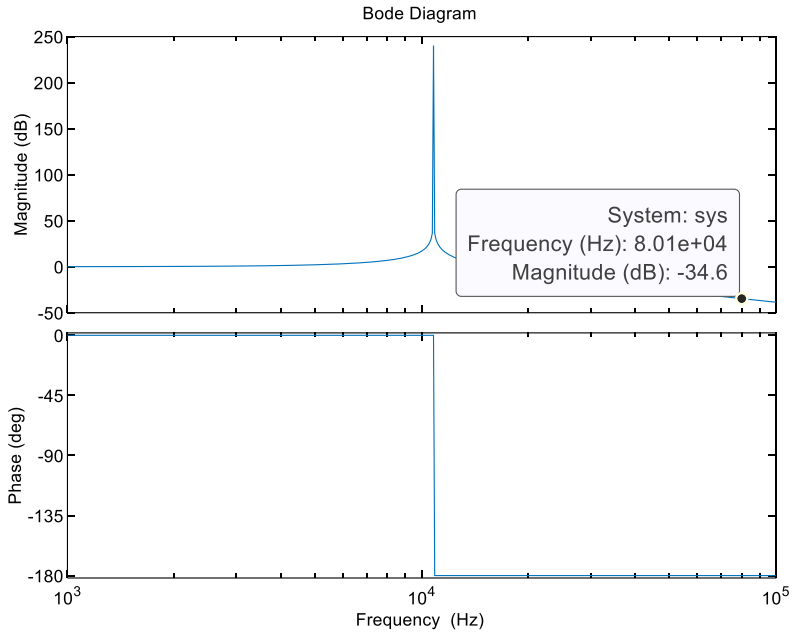

Figure 6.38: Bode diagram with C_{IN} = 162 [uF]

With this value for the capacitor C_{IN}, the attenuation maximal possible to have, is around 53,7x. The current passing through the battery would be around 3,12 [A].

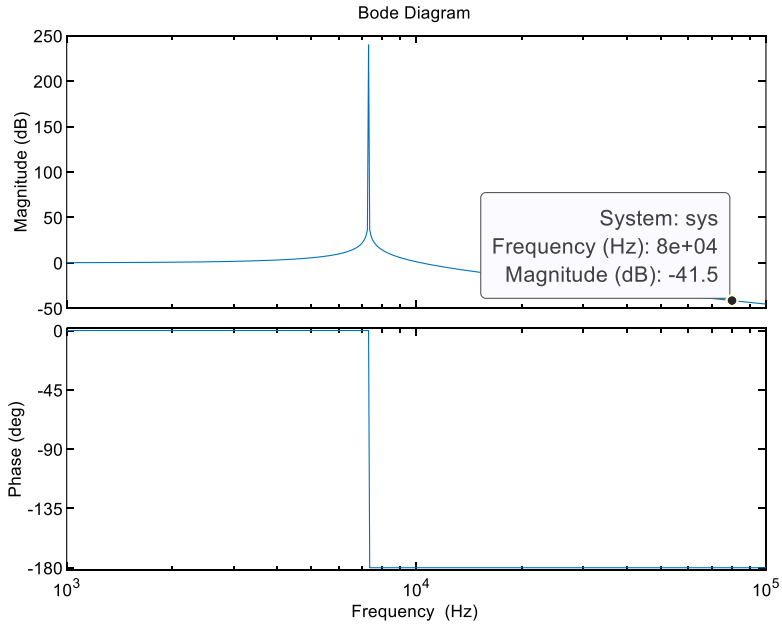

Figure 6.39: Bode diagram with C_{OUT} = 72 [uF]

In the second bridge, the attenuation will be around 118x with the value of C_{OUT}, giving a current around 470 [mA].

Then, an analysis of the waveforms comparing the before and after the filter shows a real attenuation without the resonant problem. It means the filter is applied as wanted and reduce the DC current in both sides of the converter with big attenuations.

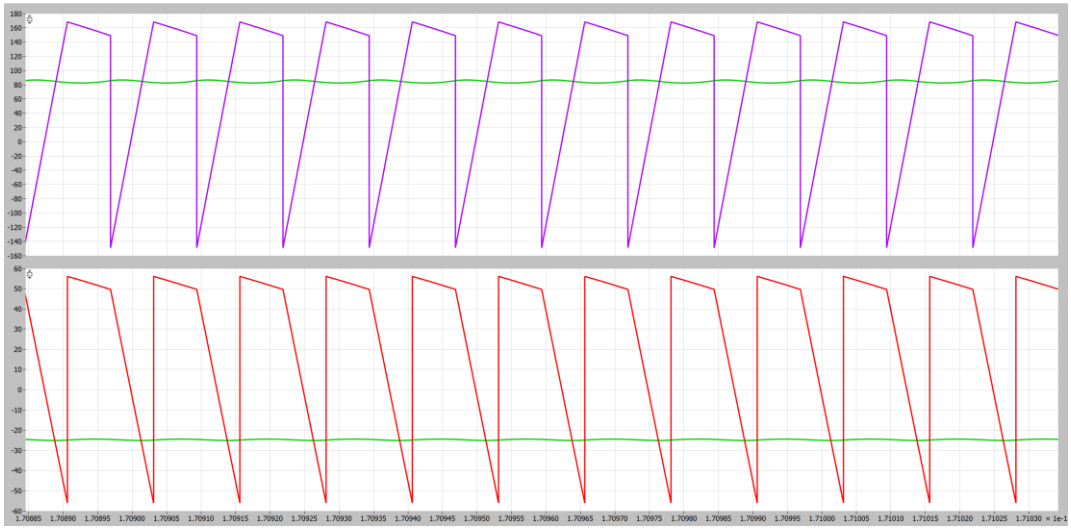

Figure 6.40: Comparison of waveforms before and after the filer with final capacitors choice

A deeper analysis can be made with a FFP representation of the harmonics. As said previously, the multiple of the frequency used for the filter were excited. By changing the value of the capacitors in order filter the signal the most possible and avoiding the excitation peak there is with this model of filter, the following harmonics of the frequency have been attenuated as well. The Figure 6.41 shows those attenuations on the harmonics.

Figure 6.41: FFP graphic of harmonics attenuations

As visible, all harmonics are attenuated in a high factor. A control of the attenuation's factors can be made with this graphic of the simulated filters. The graphic above represents the filter in the primary, and by taking the values measured before I_V and after I_m attenuation in the first harmonic, the factor of attenuation can be calculated as:

$$\mu_1 = \frac{I_{m1}}{I_{V1}} = \frac{116{,}66}{2{,}13} = 54{,}76x \tag{26}$$

$$\mu_2 = \frac{I_{m2}}{I_{V2}} = \frac{41{,}08}{0{,}33} = 124{,}48x \tag{27}$$

The factors of attenuation are quite similar to the one expected before.

6.7.3.5 Choice of the semiconductors

The choice of semiconductors is designed to fulfil the required objectives. That means, being able to provide work with the least amount of losses to guarantee the notions of power density and high conversion efficiency. Based on the thermal analyses performed for each pre-selected semiconductor, the choice is based on a series of criteria.

- Low switching losses
- Low conductions losses
- Maximal junction temperature up to 100 [°C]
- Maximal heatsink temperature up to 65 [°C]
- Supplier stock big enough
- Low semiconductor unit price

These criteria therefore include the pre-selection, especially from a logistical point of view, and consider the elements measured during the modelling which clarify certain elements of the pre-selection such as the different losses.

As the temperatures are proportional to the total losses, the loss criteria do not need to be considered twice. As well, as the radiator temperature is also proportional to the junction temperature, the criteria resulting from the thermal analyses can be grouped under one criterion such as the junction temperature. The choice of components is therefore made by comparing all the semiconductors with the logistics criteria and the temperature criterion. However, the weight given to each factor is not the same. The technical criterion of temperature is much more important than the other two, as it is an element that does not vary over time and is directly related to the efficiency of the converter. Therefore, subjective weights are put on each category; a weight of 5 for the junction temperature, a weight of 2 for the component stock, being important for the development of the converter, and a weight of 1 for the component price.

The final comparison of the components according to the criteria is therefore as follows:

	First Bridge in Parallel			Second Bridge					
With Equation	**Microchip - MSC015SMA070B**	**Infineon - IPW60R017C7XKSA1**	**IXYS - IXTK120N65X2**	**ONSEMI - NTHL020N120SC1**	**Wolfspeed - C3M0016120D**	**Microchip - MSC017SMA120B**	**Wolfspeed - C3M0021120D**	**Microchip - MSC025SMA120B**	**UnitedSiC - UF3SC120016K3S**
Technology	SiC	Si	Si	SiC	SiC	SiC	SiC	SiC	SiC
Vds [V]	700,00	600,00	650,00	1200,00	1200,00	1200,00	1200,00	1200,00	1200,00
Id [A]	140,00	109,00	120,00	103,00	115,00	113,00	100,00	103,00	107,00
Rds(on) [mΩ]	19,00	17,00	23,00	28,00	22,30	22,00	28,80	31,00	21,00
5 - Junction Temperature [°C]	82,10	81,20	81,20	59,80	57,70	57,70	60,90	56,80	56,40
2 - Stock [pce]	162,00	736,00	57,00	0,00	1255,00	211,00	164,00	528,00	424,00
1 - Price [€]	36,80	29,88	23,00	53,04	82,05	47,91	36,92	41,30	52,99
	44%	**63%**	**42%**	**46%**	**68%**	**52%**	**52%**	**59%**	**56%**

Table 15: Final comparison with equation's method

The first comparison above demonstrates the results obtained with the equation-modelled semiconductors, Table 15.

For the first bridge, the differences are mainly in the stock criterion. This is why the semiconductor of the manufacturer "Infineon" makes the difference. In terms of temperature, all three are relatively similar and the price is higher for the SiC technology. Nevertheless, the choice is not necessarily made on the basis of the indicative comparison percentage at the bottom of the table. The technology criterion can be added to the reflection. Indeed, at first glance, the semiconductor with the highest percentage should be chosen. However, given that the technology used for the second bridge is "SiC" and for the sake of simplifying the control of the semiconductor, which could be carried out in the same way on both bridges, the semiconductor of the manufacturer "Microchip" is more interesting. Especially since the technical results regarding losses are the same and the stock is sufficient for the realization of this converter.

For the second bridge, the results are relatively similar for each of the semiconductors listed, as the temperature, the most important weight in the comparison, is relatively similar. Again, the stock favours a semiconductor, especially the first one from the manufacturer "Wolfspeed". In order to refine the choice, the second modelling method has the power to vary the results greatly.

	First Bridge in Parallel			Second Bridge					
With Graphic	**Microchip - MSC015SMA070B**	**Infineon - IPW60R017C7XKSA1**	**IXYS - IXTK120N65X2**	**ONSEMI - NTHL020N120SC1**	**Wolfspeed - C3M0016120D**	**Microchip - MSC017SMA120B**	**Wolfspeed - C3M0021120D**	**Microchip - MSC025SMA120B**	**UnitedSiC - UF3SC120016K3S**
Technology	SiC	Si	Si	SiC	SiC	SiC	SiC	SiC	SiC
Vds [V]	700,00	600,00	650,00	1200,00	1200,00	1200,00	1200,00	1200,00	1200,00
Id [A]	140,00	109,00	120,00	103,00	115,00	113,00	100,00	103,00	107,00
Rds(on) [mΩ]	19,00	17,00	23,00	28,00	22,30	22,00	28,80	31,00	21,00
5 - Junction Temperature [°C]	94,95	-	-	156,90	114,40	178,66	131,00	87,10	74,10
2 - Stock [pce]	162,00	736,00	57,00	0,00	1255,00	211,00	164,00	528,00	424,00
1 - Price [€]	36,80	29,88	23,00	53,04	82,05	47,91	36,92	41,30	52,99
	39%	-	-	**8%**	**46%**	**4%**	**23%**	**47%**	**49%**

Table 16: Final comparison with graphic's method

The second comparison, above, demonstrates the results with the graphical modelling method, Table 16.

For the first bridge, only the semiconductor made with "SiC" technology gives a result. This is why the final choice of component type for the first bridge is based on the first comparison and not on this one, which does not give a comparison between each component.

For the second bridge, the results are more diverse. Four components can already be excluded from the final choice, as they exceed the prescribed safety limits in terms of temperature. The choice is therefore between the last two semiconductors in the table, i.e., between the second from the manufacturer "Microchip" and the one from "UnitedSiC". The technical criteria will take precedence over the logistical criteria, which are more favourable to the first. However, the temperature margin in relation to the limit is greater and the indication that the power losses are lower in the second semiconductor favours the second in the final choice.

6.7.3.5.1 Final choice of semiconductors

In all these comparisons of results, the choice of the second modelling method, the graphical one, should generally take precedence over the final decision. The reason is that the data given by the manufacturers is measured in the laboratory and gives a more accurate result when modelling. On the other hand, when manufacturers do not provide this information, the equation method is used to get as close as possible to the reality of the component. According to the results, the formula gives a result quite similar to the manufacturer's data, but in other cases large differences are observed. It would therefore be interesting to study this equation more precisely in order to optimise it.

In the current case of the study, the components of the first bridge have to be defined by the analytical method. As described in the comparison of the results with this method, the choice gives an advantage to the component made with the "SiC" technology, i.e., the component of the manufacturer "Microchip" whose model is "MSC015SMA070B". This choice allows a globalization of the technology for the power devices on the whole converter. As it is a double parallel circuit, to reduce costs, this first bridge needs eight semiconductors at a price of 36,80 [€]. A total price of 294,40 [€] for the realisation of this first bridge.

The final choice for the components of the second bridge is based on the other, more precise method, which gives reason to the semiconductor of the manufacturer "UnitedSiC" whose model is "UF3SC120016K3S". The simple assembly is sufficient for this second bridge, and only four components are needed at a price of 52,99 [€]. A total price of 211,96 [€] for the realisation of the second bridge.

6.8 Global analysis of the development

The purpose of the overall analysis of the converter is to define whether all the elements fit together so that the converter can evolve in the specified application. In addition, once all the components have been chosen and sized, it is important to check that the objectives requested at the outset are achieved. As a reminder, the converter is added to a smart grid which consists directly in being a tool to achieve the European strategies in terms of energy use. This means that if the objective is to waste as little as possible, it is necessary to be able to develop efficient equipment from the outset. In addition to the specific objectives of the environment in which the converter operates, which have been used for the dimensioning of the components, a series of additional conditions have to be analysed on the converter.

- Galvanic isolation
- Bidirectional power flow capability
- High conversion efficiency (η > 95 % at the nominal operating point)
- High power density
- Autonomous cooling

If galvanic isolation is already guaranteed by the integration of a transformer in the heart of the converter, if bidirectionality is possible by the chosen Dual Active Bridge topology and if autonomous cooling is ensured by the previously dimensioned radiators and fans, its high conversion efficiency and its high-power density are two notions that still need to be verified.

6.8.1 Efficiency of the converter

The efficiency of the inverter is an important requirement. The higher the efficiency, the more efficient it is. Each time elements are added to the network to transform the energy, losses occur. The objective is to develop tools that have a minimal impact on the network. This is why this notion of efficiency must be calculated to validate the converter. The efficiency equation is as follows:

$$\eta = \frac{P_{out} - P_{th}}{P_{in}} \tag{28}$$

The electrical powers at the input and at the output are relatively the same because it is transferred through the converter. To calculate the efficiency of this converter, the power devices losses simulated generate a total heat flow dissipated in the two heatsinks. These heat flows, which represent almost the total of the power losses of this converter, have to be subtracted to the output power. Indeed, some other losses generated by the magnetic field of transformer and some other components not especially studied in this work should be considered as well. But the main power losses of this converter are generated by the studied field of this work and can be considered as all the power losses. Then the efficiency is calculated by comparing the input power with output power reduced by the power losses described.

Pin [W]	**Pout [W]**	**Pth1 [W]**	**Pth2 [W]**	**Pth [W]**
19902,60	19902,00	340,25	127,42	467,47

Table 17: Powers measured on the simulation

$$\eta = \frac{19902{,}00 - 467{,}47}{19902{,}60} = 97{,}65\ [\%] \tag{29}$$

The efficiency of this converter is validating the objectives given at the beginning of the work in being more than 95%. This converter is optimized to have the least losses possible and complete the goals of high efficiency.

6.8.2 Space taken for the converter

Based on the project [3], the converter size enters in a rack of 360x230x200 [mm]. This rack can be slipped into a special cupboard. This size is relatively small for the power it can be transferred. Its volume can be calculated as:

$$V = 360 * 230 * 200 = 16{,}56\ [dm^3] \tag{30}$$

This volume is useful to define the power density of the converter.

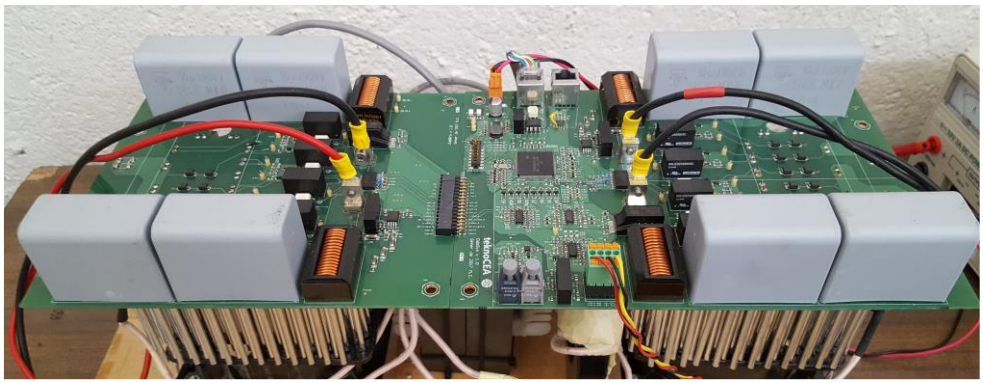

Table 18: Picture of the converter used for the project RESOLVD

6.8.3 Results of the power density

The power density is relative to the quantity of power which can possibly be transferred through the converter in specified volume. It is interesting that converter is as small as possible, and a high quantity of power can pass through. This power density can be estimated as:

$$Pd = \frac{19{,}90 - 0{,}47}{16{,}56} = 1{,}17\ [\frac{kW}{dm^3}] \tag{31}$$

This power density in this converter is not the best possible for a converter. Indeed, nowadays, converters can reach density 30 times bigger than this (31). Depending on the use this criterion is really important, for example in EVs. However more the power density is important, more the price of the converter increase. For the application of this converter, it is possible place this in a cupboard in a building dedicated for this purpose. The power density is then not an imperative point.

6.8.4 Budget for components studied

In order to represent how much could be the material cost of the component studied, especially for the DAB topology and the filters, of this work, this table below represents the prices of all components choose to realize this converter.

Component	**Unit price [€]**	**Total price [€]**
MOSFETs first bridge	36,80	294,40
MOSFETs second bridge	52,99	211,96
Insulator	115,14	115,14
Heatsinks	63,00	126,00
Fans	28,13	112,52
Inductances IN LC filter	32,86	65,72
Inductances OUT LC filter	33,63	67,26
Capacitor IN LC filter	15,80	15,80
Capacitor OUT LC filter	11,83	11,83
	TOTAL :	**1020,63**

Table 19: Budget for components studied

The price was one of the criteria to choose the component, this proposal of component corresponds to the most efficient one studied with the lowest price possible. At the moment of the thesis stocks are available for these components (data base July 2022) but the market is evolving quick, and quantity of these products could vary.

7 Methodology

The methodology of this thesis is based on a structure of scientific research. This structure answers to the goals presented in Chapter 3. It consists of understanding these objectives and the application where this work has to been applied, and then prepare a planning of work supposed to complete the research which as to be investigated. Then the work structure is separated on two big blocks which consist in make a state of the art of the subject to understand the environment of the work and next realize the research, analyses, and control of the work, to finally propose a sizing corresponding to the demand.

7.1 Gantt planning

An initial Gantt planning has been made in order to complete the supposed work that has to be done. On the base of this planning, research have been carried out and then software analyses have been made to simulate the studied models and start a sizing of the converter. During the work, the planning has varied depending on the new research or importance on some subjects which have been necessary to be made before others.

The Gantt corresponding to this thesis is available in Appendix B.

7.2 Hypothetic budget

Considering this thesis as an engineering project a hypothetic budget can be made to see what could cost such a work. Indeed, the conditions in which this project has been done are particularly good if considering the state of student for using some software benefiting of special versions which make the cost lower. This hypothetic budget would consider this work made by an engineer in a company without student advantages. Furthermore, this work is especially made on software and the hardware part to create the converter is not started. A last point, this thesis has been made in Spain, the price of an engineer student is therefore relative to the Spanish market.

In order to sum the total amount necessary to represent this project, the costs have been divided in different categories (hardware, electricity, licenses, and labor).

7.2.1 Hardware

During this work, a personal computer (PC) has been used, a Microsoft Surface Book 2. In terms of money, the personal computer is about 2200 [€]. It is the only computer used for this work so the total amount for hardware is:

$$Hardware = PC = 2200{,}00\ [€] \tag{32}$$

7.2.2 Electricity

A personal laptop as described before, in terms of electricity, consume around 80 [W]. Considering the computer has been running the total duration of the project, around 600 [h] the total amount for electricity use, with a price of 0,25 [€/kWh], is:

$$Electricity = N_{Hours} * Power *= 80W * 600h * \frac{0{,}25€}{\text{kWh}} = 12{,}00\ [€] \tag{32}$$

7.2.3 Licenses

Different software has been used during this thesis. Especially, MatLab Simulink, PLECS and Microsoft Office Excel. MatLab license is around 840 [€/year]. PLECS has an offer for its annual license at 1300 [€/year]. Microsoft Office Excel has an offer of 7 [€/month]. Considering this project spread on different moths, the yearly cost for licenses is choose.

$$MatLab \ = 840\,€/year * \ 1\ \text{year} = 840{,}00\ [€] \tag{33}$$

$$PLECS = 1300\,€/year * \ 1\ \text{year} = 1300{,}00\ [€] \tag{34}$$

$$Excel = 7\,€/month * \ 12\ \text{months} = 84{,}00\ [€] \tag{35}$$

$$Licenses = MatLab + PLECS + Escel = 840 + 1300 + 84 = 2224{,}00\ [€] \tag{36}$$

7.2.4 Labor

It is important to take into consideration the hours the engineer student has spent, with a price per hour fixed at 40 [[€/h].

$$Engineer\ _{Student} = 40\,€/h * \ 600\ \text{h} = 24'000{,}00\ [€] \tag{37}$$

7.2.5 Total cost

The total cost of this hypothetic budget adds up all the previous cost and define the cost of this project.

$$Total_{Cost} = Hardware + Electricity + Licenses + Labor \tag{38}$$

$$Total_{Cost} = 2200{,}00 + 12{,}00 + 2224{,}00 + 24000{,}00 = 28'436{,}00\ [€] \tag{39}$$

8 Conclusions

In this thesis an investigation is carried out, based on an existing project [3], in order to be able to adapt an isolated bi-directional DC converter (IBDC) for a specific application that has been defined in chapter 4. Thus, the requirements for this converter, which concerns the charging and discharging of a battery in a smart grid, have to be fulfilled. The main objective is defined as the study of the design of different topologies of IBDCs, its dimensioning and analysis. A special focus is put on the research and analysis of losses in the different power devices, with the aim to optimise the existing project converter in this respect. The main focus is on the semiconductors, which are a source of losses for the converter. These elements, being necessary for the realisation of converters, are part of a particularly unstable market at the moment and therefore require an adaptation of the design method of the conversion electronics, directly linked to the various suppliers of the market.

This thesis is divided into different chapters that structure the work and the method used for the study of this converter. The following sections outline the results of these chapters.

8.1 Chapter 4 : Application and its specifications

This chapter introduces the environment in which the converter should evolve. Indeed, this converter is a rework of an existing project [3], but can be found in different environments. In addition, the converter under study is intended to be the conversion device that allows a power transfer between an HV DC Bus and an LV DC Bus to which a battery is connected. This battery allows to be a back-up element in case of power failure and also a stabilisation element of network disturbances.

Next, environmental specifications are given, in terms of the desired transfer power (20 [kW]) and the voltage level of the buses. Also, additional conditions are described as necessary for an IBDC, such as galvanic isolation, high power density or high efficiency.

This chapter sets the scene for the following study to be able to meet these requirements. The following decisions on the design of components for this converter are based on this chapter.

8.2 Chapter 5 : State of the Art

The aim of this chapter is to present some existing IBDC topologies that could be used for the realisation of the converter related to the previously presented application. Dual-Stage (2-S) and Single-Stage (1-S) topologies are presented, based on [4].The (1-S) topology is preferred to the (2-S) because it has a single converter for power transfer. Several sub-topologies of the (1-S) are presented and categorized into three groups: low number of switches, Dual Bridge without resonant network and Resonant DAB. Each group is described with different circuit examples. The category with the lowest number of switches includes circuits such as flyback and forward. The Dual Bridge without resonant network includes circuit topologies such as Dual Active Bridge (DAB) and different variations. The last category contains circuits such as LLC or LCC.

From this comparison of different topologies, a choice for the converter to be implemented has to be made. The category with the lowest number of switches is suitable for applications up to 2 [kW] but cannot be chosen for the desired application with a power transfer of 20 [kW]. The last category is relatively limited due to restrictions on voltage peaks and short

circuits. The choice should therefore be made in the category of Dual Bridges without resonant networks. The Dual Active Bridge (DAB) is chosen in this category because of its low component count and the possibility of soft switching.

8.3 Chapter 6 : The DAB converter

This chapter is the most important one of the works. It is divided into different steps:

- The study of the topology of the DAB converter
- The study of the simplified lossless model
- The study of the different losses generated by the power switching devices
- Study of the switching modes
- Definition of the converter modulation
- Sizing of the components
- Overall analysis of the converter

The first four steps include a global study of the converter and define the basis on which the following steps are carried out. In particular, the identification of the different losses, such as the most important ones like switching losses and conduction losses are taken into account for the optimisation of the sizing of the power components.

The modulation scheme of the converter is defined as Single-Phase Shift Modulation for its simplicity of control based on a single-phase shift angle. As the aim of the project is to optimise the switching devices, more complex modulations to reduce the losses of the converter are not required to be studied. Also, the value of the leakage inductance required for this modulation is defined, as well as the current flowing through it.

The sizing of the components is based on the environment described by the previous choices and studies. The components studied in this work are the semiconductors allowing the switches for the modulation, the components necessary for the dissipation of losses and the components allowing the implementation of filters. A first selection of components is made according to market availability. A selection of semiconductors compares different technical characteristics, such as loss potential, and logistical characteristics, such as price, stock, and lead time. This comparison gives an advantage to some over others. In order to validate this selection, a simulation analysis is conducted. To simulate these components, a model of each of them has to be made. This modelling requires an understanding of the loss concepts previously studied in order to create models corresponding to the components described by the suppliers.

The thermal analysis of semiconductors is the main focus of this thesis. A series of commercially available semiconductors are analysed with models performed analytically and graphically according to the manufacturers' data. Differences are noticed and are the subject of potential future work to be studied. Semiconductors are finally chosen to fulfil the function required for this converter. The choices are made on the base of the lowest losses emitted, which means a low temperature measured at the semiconductor, the available stock in the market and a relatively low price of the component.

The analysis in which they have been studied also takes into account all the devices needed to dissipate these losses such as radiators, fans, or other elements.

An additional study of the inverter filters is carried out to ensure lower current upstream and downstream of the inverter. An attenuation of the harmonics generated by the converter is achieved by adding these filters.

A list of the result of choices made for all the component studied is established after all analyses. It is made on the basis of comparison between the first selection and the results of the thermal analysis.

Finally, a global analysis of the converter is carried out, checking if the objectives presented at the beginning are reached and also defining the cost of the components studied during this chapter.

8.4 Chapter 7 : Methodology

This chapter presents the methodology used for this thesis. It presents the Gantt plan defined for this work. Also, a hypothetical budget is presented to have a financial point of view of what such a study represents.

8.5 Future work

Various future works can be carried out based on this thesis. For example, the study of the use of this type of converter in this kind of application with backup battery for just-in-time consumption. In other words, to have a network that is full of parasitic production elements (wind turbines, solar panels) being extremely disturbed and that is continuously stabilised by this device which is very fast. It should also be examined whether such a just-in-time solution would make it possible to reduce the quantity of batteries, which are larger and intended purely for storage. Knowing the ecological impact that these batteries have on the environment, it would be interesting to define which solution would reduce it the most.

A second study that can be carried out as a result of this thesis concerns the modelling of semiconductors, more specifically with SiC technology. During this work a difference was perceived between analytical modelling by equation and graphical modelling based on manufacturers' data. It would be interesting to optimise the analytical modelling to define an equation that is as close as possible to the globality of the semiconductors offered on the market. It is certain that the equations used for the modelling of this work are not complete for SiC technology.

8.6 Overall conclusion

This overall conclusion of the presented thesis is that Dual Active Bridge (DAB) converter is suitable for the realization of Isolated Bidirectional DC converter in the application of conversion organ between a HV DC Bus of smart grid and LV DC Bus used for a back-up battery. It fulfil the converter requirements, as galvanic isolation or bidirectionality, which are related to a transfer power of 20 [kW].

This work ends with interesting results for the optimisation of power devices. Indeed, they depend mostly on the state of the actual market but have completed the objectives given at the beginning. The way to classify which components are adapted for the application, in doing a first selection from manufacturers' data and then in doing simulation's analyses, to finally combine each other in a global comparison, allows a best selection. Especially when the market is unstable, as it is during the thesis, developments need to continue depending on what is available from manufacturer.

In a personal point of view, this subject was a first try in the development of such converter. Many things were new and have been well understood with the studies investigated on this topology of Dual Active Bridge. The possibility of additional knowledge is wide, knowing the different modulation possible with this topology. Power losses can be reduced much more with different aspects not evaluated in this thesis and this means further works are possible in this topic.

Bibliography

[1] European Commission. A European Green Deal: General website (Last accessed: 06.09.2022). [Online]. Available: https://ec.europa.eu/info/strategy/priorities-2019-2024/european-green-deal_en

[2] European Commission. The REPowerEU Plan: General website (Last accessed: 06.09.2022). [Online]. Available: https://ec.europa.eu/info/strategy/priorities-2019-2024/european-green-deal/repowereu-affordable-secure-and-sustainable-energy-europe_fr

[3] RESOLVD project. Euopean Union's Horizon 2020, LCE-01-2016-2017. [Online]. Available: https://resolvd.eu/

[4] Macià Capó-Lliteras. Design optimization of galvanically isolated DC-DC converters, PhD Proposal. Available: CITCEA-UPC internal document.

[5] Jordi Everts. Modeling and Optimization of Bidirectional Dual Active Bridge AC-DC Converter Topologies. PhD Thesis.

[6] G. G. Oggier, G. O. GarcÍa and A. R. Oliva, "Switching Control Strategy to Minimize Dual Active Bridge Converter Losses," in IEEE Transactions on Power Electronics, vol. 24, no. 7, pp. 1826-1838, July 2009, doi: 10.1109/TPEL.2009.2020902.

[7] Microchip. MOSFET MSC015SMA070, Datasheet. [Online]. Available: https://www.mouser.es/ProductDetail/Microchip-Technology-Atmel/MSC015SMA070B?qs=MLItCLRbWsywu9VMuYVdUQ%3D%3D

[8] Infineon. MOSFET IPW60R017C7XKSA1, Datasheet. [Online]. Available: https://www.mouser.es/ProductDetail/Infineon-Technologies/IPW60R017C7XKSA1?qs=Qyx3PVvfm65k%252B8GuzV67%2FA%3D%3D

[9] IXYS. MOSFET IXTK120N65X2, Datasheet. [Online]. Available: https://www.mouser.es/ProductDetail/IXYS/IXTK120N65X2?qs=uwxL4vQweFO18Hnyu5EO4Q%3D%3D

[10] ONSEMI. MOSFET NTHL020N120SC1, Datasheet. [Online]. Available: https://www.mouser.fr/ProductDetail/onsemi/NTHL020N120SC1?qs=xZ%2FP%252Ba9zWqb7NxC9etpTeQ%3D%3D

[11] Wolfspeed. MOSFET C3M0016120D, Datasheet. [Online]. Available: https://www.mouser.fr/ProductDetail/Wolfspeed/C3M0016120D?qs=BJlw7L4Cy7%2Fxox9rryyk%2FA%3D%3D

[12] Microchip. MOSFET MSC017SMA120B, Datasheet. [Online]. Available: https://www.mouser.fr/ProductDetail/Microchip-Technology/MSC017SMA120B?qs=TuK3vfAjtkWYCqEvfsNDOg%3D%3D

[13] Wolfspeed. MOSFET C3M0021120D, Datasheet. [Online]. Available: https://www.mouser.fr/ProductDetail/Wolfspeed/C3M0021120D?qs=BJlw7L4Cy7%252BrfIp%2FrFfUDA%3D%3D

[14] Microchip. MOSFET MSC025SMA120B, Datasheet. [Online]. Available: https://www.mouser.fr/ProductDetail/Microchip-Technology/MSC025SMA120B?qs=MLItCLRbWsxDOUaqiyUI3w%3D%3D

[15] UnitedSiC. MOSFET UF3SC120016K3S, Datasheet. [Online]. Available: https://www.mouser.fr/ProductDetail/UnitedSiC/UF3SC120016K3S?qs=Cb2nCFKsA8oH619YF8NzqQ%3D%3D

[16] Gabriel Gross. Cálculo de pérdidas en semiconductors. 2018-03-15. Available: CITCEA-UPC internal document.

[17] Bergquist. Insulator film, Datasheet. [Online]. Available: https://es.rs-online.com/web/p/almohadillas-termicas/0127013/

[18] Vishay. Inductances LC filter IHXL1500VZEBR68M5A, Datasheet. [Online]. Available: https://www.mouser.es/ProductDetail/Vishay-Dale/IHXL1500VZEBR68M5A?qs=IS%252B4QmGtzzrHJdkWpOwiRg%3D%3D

[19] Vishay. Inductances LC filter IHXL1500VZEB3R3M5A, Datasheet. [Online]. Available: https://www.mouser.es/ProductDetail/Vishay-Dale/IHXL1500VZEB3R3M5A?qs=IS%252B4QmGtzzr16ePzKoUUfw%3D%3D

[20] Kyocera AVX. Capacitor LC filter FFB54H0276KJC, Datasheet. [Online]. Available: https://www.mouser.es/ProductDetail/Kyocera-AVX/FFB54H0276KJC?qs=Qb7MlAwYWrdS6gG1Hx8xWw%3D%3D

[21] Vishay. Capacitor LC filter MKP1848620704P4, Datasheet. [Online]. Available: https://www.mouser.es/ProductDetail/Vishay-Roederstein/MKP1848620704P4?qs=i2mp%2Fn9EmlL2rtwZePAUvQ%3D%3D

[22] Guash. Heatsinks RG42080L24/110RM, Datasheet. [Online]. Available: https://www.e-guasch.com/es/power-electronics-items/disipador-alta-eficiencia/

[23] Sanyo Denki. Fans 9G0824G101, Datasheet. [Online]. Available: https://products.sanyodenki.com/en/sanace/dc/dc-fan/9G0824G101/

[24] Aavid Thermalloy Thermal Seminar," Mustafa, S., El Segundo, CA, November 2002.

[25] Zhenyu Wang and Alberto Castellazzi. Device loss model of a fully SiC based dual active bridge considering the effect of synchronous rectification and deadtime. Proceedings - 2017 IEEE Southern Power Electronics. Conference, SPEC 2017, 2018-Janua:1–7, 2018. 39

Appendix A

Measures of software simulation of semiconductors:

		First Bridge			Second Bridge					
Tamb = 45 [°C]		**Microchip - MSC015SMA070B**	**Infineon - IPW60R017C7XKSA1**	**IXYS - IXTK120N65X2**	**ONSEMI - NTHL020N120SC1**	**Wolfspeed - C3M0016120D**	**Microchip - MSC017SMA120B**	**Wolfspeed - C3M0021120D**	**Microchip - MSC025SMA120B**	**UnitedSiC - UF3SC120016K3S**
Not in parallel With equation	**Junction Temperature [°C]**	176,16	158,32	161,30	59,80	57,70	57,70	60,90	56,80	56,40
	Heat Sink Temperature [°C]	75,90	71,50	77,70	49,50	48,50	48,52	49,40	48,40	48,10
	MOSFET Conduction Loss [W]	135,30	117,70	145,90	17,70	15,95	15,95	19,90	14,60	14,20
	DIODE Conduction Loss [W]	7,16	3,60	3,60	2,90	0,00	0,07	0,24	0,89	0,05
	MOSFET Switching Loss [W]	4,00E-04	6,00E-04	9,00E-04	3,00E-04	6,40E-04	2,50E-04	9,80E-04	3,30E-04	4,00E-04
	DIODE Switching Loss [W]	2,60E-05	4,00E-04	6,00E-04	3,30E-06	1,00E-05	7,60E-06	1,80E-05	1,20E-05	6,70E-06
	Heat Flow [W]	563,00	477,00	592,30	82,50	63,70	64,00	80,60	62,00	57,25
Not in parallel With graphic	**Junction Temperature [°C]**	176,90	-	-	182,10	114,40	178,66	131,00	87,10	74,10
	Heat Sink Temperature [°C]	82,60	-	-	76,40	64,16	81,88	68,70	56,80	51,98
	MOSFET Conduction Loss [W]	135,30	-	-	17,80	15,96	15,95	19,90	14,60	14,20
	DIODE Conduction Loss [W]	7,20	-	-	2,60	0,00	0,07	0,25	0,86	0,06
	MOSFET Switching Loss [W]	29,40	-	-	121,80	71,13	151,60	88,50	38,00	17,54
	DIODE Switching Loss [W]	2,60E-05	-	-	4,00E-01	1,00E-05	7,60E-06	1,28E-05	1,20E-05	6,70E-06
	Heat Flow [W]	682,70	-	-	571,20	348,40	670,00	431,80	214,00	126,90
In parallel With equation	**Junction Temperature [°C]**	82,10	81,20	81,20	-	-	-	-	-	-
	Heat Sink Temperature [°C]	58,80	58,60	60,90	-	-	-	-	-	-
	MOSFET Conduction Loss [W]	31,40	30,70	35,60	-	-	-	-	-	-
	DIODE Conduction Loss [W]	0,68	0,81	0,75	-	-	-	-	-	-
	MOSFET Switching Loss [W]	2,00E-04	4,00E-04	5,50E-04	-	-	-	-	-	-
	DIODE Switching Loss [W]	1,30E-05	4,00E-04	6,40E-04	-	-	-	-	-	-
	Heat Flow [W]	252,80	247,20	288,40	-	-	-	-	-	-
In parallel With graphic	**Junction Temperature [°C]**	94,55	-	-	-	-	-	-	-	-
	Heat Sink Temperature [°C]	63,46	-	-	-	-	-	-	-	-
	MOSFET Conduction Loss [W]	31,43	-	-	-	-	-	-	-	-
	DIODE Conduction Loss [W]	0,68	-	-	-	-	-	-	-	-
	MOSFET Switching Loss [W]	10,90	-	-	-	-	-	-	-	-
	DIODE Switching Loss [W]	1,32E-05	-	-	-	-	-	-	-	-
	Heat Flow [W]	335,64	-	-	-	-	-	-	-	-

Appendix B

Gantt planning of the project: